IMAGING THE EARTH's INTERIOR

Jon F. Clærbout
Cecil and Ida Green Professor of Geophysics
Stanford University

email: jon@sep.stanford.edu

This book is dedicated to Cecil Green
who enjoyed the excitement of being among the pioneers,
had the foresight to garner a fortune,
and how has the fun of giving it
to universities throughout the world.

©January 31, 1996

Contents

1 Introduction to imaging **1**

1.1 EXPLODING REFLECTORS 1

1.2 SURROUNDING DISCIPLINES 13

2 Discrete Fourier transform **25**

2.1 FT AS AN INVERTIBLE MATRIX 25

2.2 INVERTIBLE SLOW FT PROGRAM 27

2.3 SETTING UP THE FAST FOURIER TRANSFORM 29

2.4 TWO-DIMENSIONAL FT 32

3 Wide-angle migration methods **39**

3.1 PLANE-WAVE SUPERPOSITION 39

3.2 SUMMATION AND SUPERPOSITION OF CONICS 46

3.3 THE PHASE-SHIFT METHOD 50

3.4 THE STOLT METHOD 53

3.5 INFLUENCES ON MIGRATION QUALITY 57

3.6 THE PARAXIAL WAVE EQUATION 63

4 Migration by finite differences **73**

4.1 WAVE-EXTRAPOLATION EQUATIONS 74

4.2 FINITE DIFFERENCING 84

4.3 WAVEMOVIE PROGRAM 94

4.4 MIGRATION IN THE (omega,x)-DOMAIN (KJ) 103

5 Splitting and working in the time domain **107**

5.1 SPLITTING AND FULL SEPARATION 108

5.2 RECURSIVE DIP FILTERS 116

5.3 RETARDED COORDINATES 120
5.4 FINITE DIFFERENCING IN (t, x, z)-SPACE 124
5.5 INTRODUCTION TO STABILITY 131

6 Offset, another dimension **135**
6.1 ABSORPTION AND A LITTLE FOCUSING 143
6.2 INTRODUCTION TO DIP 149
6.3 SURVEY SINKING WITH THE DOUBLE-SQUARE-ROOT EQUATION 161
6.4 THE MEANING OF THE DSR EQUATION 171

7 Velocity and dip moveout **181**
7.1 STACKING AND VELOCITY ANALYSIS 181
7.2 MIGRATION WITH VELOCITY ESTIMATION 196
7.3 LATERAL VELOCITY IN BIGGER DOSES 207

8 Dispersion relations **219**
8.1 COSMETIC ASPECT OF WAVE EXTRAPOLATION 221
8.2 ANISOTROPY DISPERSION IN MIGRATION 233
8.3 FREQUENCY DISPERSION IN WAVE-MIGRATION 242
8.4 ACCURACY—THE CONTRACTOR'S VIEW 252

9 The craft of wavefield extrapolation **259**
9.1 ABSORBING SIDES 259
9.2 TUNING UP FOURIER MIGRATIONS 263
9.3 IMPEDANCE 270
9.4 THE BULLETPROOFING OF MUIR AND GODFREY 286

10 Slanted waves **291**
10.1 RADIAL TRACES 293
10.2 SLANT STACK 296
10.3 SNELL WAVES AND SKEWED COORDINATES 306
10.4 INTERVAL VELOCITY BY LINEAR MOVEOUT 314

11 Multiple reflections **325**
11.1 MULTIPLE REFLECTION, CURRENT PRACTICE 325

11.2 MULTIPLE REFLECTION—PROSPECTS 341
11.3 PROFILE IMAGING 353
11.4 PREDICTIONS FOR THE NEXT DECADE 358

A RATional FORtran == Ratfor **361**

B Seplib and SEP software **363**
B.1 THE DATA CUBE 364
B.2 THE HISTORY FILE 365
B.3 MEMORY ALLOCATION 367
B.4 BASIC SUBROUTINES 368

FREEWARE, COPYRIGHT, AND PUBLIC LICENSE

This electronic book, "Imaging the Earth's Interior" is free software; you can redistribute it and/or modify it under the terms of the GNU General Public License as published by the Free Software Foundation; either version 2 of the License, or (at your option) any later version. This book is distributed in the hope that it will be useful, but WITHOUT ANY WARRANTY; without even the implied warranty of MERCHANTABILITY or FITNESS FOR A PARTICULAR PURPOSE. See the GNU General Public License for more details. You should have received a copy of the GNU General Public License along with this program; if not, write to the Free Software Foundation, Inc., 675 Massachusetts Ave., Cambridge, MA 02139, USA.

I reserve the right to distribute this book and its software for a profit. Paraphrasing The GNU General Public License, you may make modifications and copies and distribute them also, but your distribution which includes my work must be distributed free.

Jon Claerbout
January 31, 1996

Preface to network distribution

This book was originally published by Blackwell's in 1985. Only later in my next book in 1992, "Earth Sounding Analysis: Processing versus Inversion" did I understand how to make an electronic document where all the illustrations are reproducible, being recalculated from original data, parameters, and programs. I tried revising this book to bring it up to that standard, the standard of the 1992 book, however too much had been lost, indeed, many of the examples shown in this book were not done at our laboratory. When this book was declared out of print about 1992 I resolved to bring out this electronic version, almost a revision of the original and make it freely available over the internet. I have not yet learned how to make all the software conveniently downloadable from the internet. The figures in this book contain pushbuttons in the figure captions. Those 54 figure captions containing the letters [ER] point to software that is easily reproducible if you have the electronic book. Of these, 11 figures include movies. On these reproducible figures, you can dig in, change data, change parameters, or even change the theory. You then press the button in the figure caption and watch the figure rebuild itself (on UNIX based computers) to your specifications. I am particularly indebted to my colleague, Matthias Schwab, whose continuing collaboration is making possible these interactive documents on CD-ROM.

Subroutines

This book uses mathematics to explain the given runnable computer codes. The code itself is in Ratfor[1] a dialect of Fortran more suitable than standard Fortran for exposition.[2]

Preface to 1985 edition

Some History

Reflection seismologists make images of the earth's interior. Through the 1960s this was done in an ad hoc fashion. Between 1968 and 1972, I conceived and field tested a new method of image making based directly on the wave equation of physics. Previously the wave equation had been used to predict observations starting from simplified, hypothesized models. It was not used in routine data analysis. My imaging method using finite differences soon came into widespread use in the petroleum exploration industry. Many other people quickly became involved and made important improvements. The earlier ad hoc methods were reinterpreted and they too improved in the light of wave theory.

An industrial affiliates group, known as the Stanford Exploration Project (SEP), was founded at Stanford University to pursue the new developments. Of the forty-eight sponsoring organizations, many have substantial research departments of their own. Thus began the decade of the 1970s, in which much progress was made. In the 1980s progress continues to be made at a rapid pace.

The Place for This Book

This textbook was born of the need to teach the best of the many new ideas to those entering the industry. Because so many people enter geophysics from outside the field, I have kept specialized geophysical terminology to a minimum and defined everything. So this book should be useful, not only to those interested in petroleum exploration, but also to professionals in all disciplines in which waves are analyzed.

My previous book, *Fundamentals of Geophysical Data Processing* (FGDP), was published in 1976 and has recently been reissued. It covered more basic aspects of reflection seismic data processing such as Z-transforms, Fourier transforms, discrete linear system theory, matrices, statistics, and theory of the stratified earth. FGDP also introduced wave-equation imaging, but extensive supplements became necessary. The supplements evolved into this book. The two books are about ninety percent different, the ten percent overlap being necessary to keep this book fully self-contained.

[1] See Appendix A for details about Ratfor.

[2] In the summer of 1993 Dave Nichols and I and about 6 other people converted many of the operators of this book into C++.

This book provides a coherent overview of the whole field of data processing as it is used in petroleum exploration, and it is the basic textbook in exploration geophysics at Stanford University. I make no claim, however, that the book is encyclopedic in scope. Some important processes such as *deconvolution* and *statics* are lightly sketched, as are the experimental applications of *tomography,* while other techniques such as *ray tracing* (see Cerveny [1977]) and many kinds of *modeling* are omitted altogether. Regrettably, the migration literature alone has grown so large that significant contributions such as the theoretical side of Kirchhoff migration (see Berkhout[1980]) are omitted.

Organization

Seismic imaging is a subject that draws much from mathematics and physics. These subjects build one idea upon another in a logical progression. I chose to organize this book likewise. This organization favors the new student who wants to understand the material thoroughly. A detailed index and more than a hundred cross references are included to link the practical topics that a logical organization has left somewhat scattered about.

More encyclopedic, topic-oriented textbooks on reflection seismology are those of Waters [1981] and Sengbush [1983]. Books focused on petroleum prospecting that treat reflection seismology descriptively are Sheriff [1980] and Anstey [1980]. Complementary books on earthquake seismology are Aki and Richards [1980] and Kennett [1983].

I have also tried to reach readers who want to learn concepts while skimming the mathematics. Individual sections (which are lectures) carry practical and descriptive matters as far as possible before the mathematical analysis. The chapters themselves are also organized in this way, so for example, when you get to the middle of Chapter 1, you can skip forward to Chapter 2.

As it happens, waves are marvelously geometrical objects, and much can be learned with little mathematical analysis. But you should begin the book having previous familiarity with calculus, complex exponentials, and Fourier transformation.

Philosophy

There is always a gap between theory and practice. Many books give you no clue as to the size and location of the gap — even books in exploration geophysics. This gap is nothing to be embarrassed about. It represents the current life of the subject — the current life of any science. It is a moving target, and its size is a matter of opinion. So it is risky for me to tell you what works, what doesn't, what is important, and what isn't. Opinions go beyond facts. Your knowledge won't be complete if you don't know some opinions as well as the facts. You will be getting opinions as well as facts when I explain the discrepancies between theory and industrial practice, and when I explain what should work but doesn't seem to.

Thanks

This book is less my personal creation than was FGDP. I am indebted to many people. My colleagues Francis Muir and Fabio Rocca collaborated extensively in research. The following Stanford students contributed figures, exercises or ideas: David Brown, Junyee Chen, Robert Clayton, Steve Doherty, Raul Estevez, Paul Fowler, Bob Godfrey, Alfonso Gonzalez, Dave Hale, Bill Harlan, Bert Jacobs, Einar Kjartansson, Walter Lynn, Larry Morley, Dave Okaya, Richard Ottolini, Don Riley, Shuki Ronen, Dan Rothman, Chuck Sword, Jeff Thorson, John Toldi, Oz Yilmaz, and Li Zhiming. Industrial teaching helped me clarify the material in this book. Many useful ideas on presentation came from those who assisted me in industrial teaching, namely, Rob Clayton, Walt Lynn, Einar Kjartansson, Rick Ottolini, Fabio Rocca, Dave Hale, and Dan Rothman. Thanks are also due those who helped arrange the classes: Phil Hoyt, Lee Lu, Andre Lamer, Aftab Alam, Gary Latham, and Mike Graul.

JoAnn Heydron was first my secretary, and at a later date, the editor. Terri Ramey provided drafting and graphics assistance. Pat Bartz maintained order in ways too numerous to mention. I did most of the typing myself, as computerized typesetting has lightened that load and allows a more heavily revised and debugged final product. Peter Mora, Stew Levin, Dan Rothman, and Bill Harbert assisted in final proof reading.

Major thanks are due to Stanford University and the sponsoring organizations. Without them, much less would have been achieved. A list of sponsor names is given in an appendix. Many sponsors also donated data for our research. This is acknowledged in the figure caption. Many figures were based on data from a world-wide assortment prepared for academic use by Yilmaz and Cumro [1983]. Where figures were prepared by students, I have also acknowledged them in the caption. I prepared most of the figures myself often using outstanding graphics software utilities prepared by Rick Ottolini (*Tiplot*, *Movie*), Shuki Ronen (*Thplot*), Rob Clayton (*pen*), Joe Dellinger (*Ipen*), and Dave Hale (*Graph*).

Special thanks must also go to Western Electric Company, who donated the typesetting software (troff in 1985) that I used to prepare my lecture notes at Stanford. This software enabled me to go through many generations of improvements, eradicating scores of errors, rarely introducing new ones, all the while seeing (and having the students see) the material in almost final form. I am confident that this book has many fewer errors than did my previous book even after its second printing. When these lectures are in final form, I will simply mail a camera-ready copy and you my readers should have the book within eight weeks. So long. I'll see you at the SEG meeting.

Jon F. Claerbout

(autumn, 1984)

Introduction to 1985 edition

Prospecting for oil begins with seismic soundings. The echoes are processed by computer into images that reveal much geological history. Worldwide, echo sounding and image making constitute about a four-billion-dollar-per-year activity.

Meaning of the Measurements

The presence of oil and gas has little *direct* effect on seismic reflections. The volume of rock is much larger than the volume of hydrocarbon. The reflections are well correlated, however, with interfaces between various rock types. In porous rocks, the hydrocarbons are free to flow. Fluids tend to rise. The shapes of rock interfaces tell us where hydrocarbons may accumulate. The discovery of oil and gas in the middle of the North Sea is a remarkable success story for the reflection seismic method. As the first exploratory wells, located by reflection seismology, were being drilled, it was impossible to predict whether they would hit oil. But if oil was to be found anywhere under the North Sea, there was great confidence that these initial drill sites were much more favorable than random locations. And as it turned out, of course, oil was soon found.

After a well has been drilled and logged, the reflection images become even more valuable, because then it is known what rock type corresponds to each echo. Seismology is usually able to provide a remarkably accurate mapping of rock types at some distance from the well. It is particularly valuable to know in which direction the rocks tilt upward, and where the strata are broken by faults. Seismology provides this information at a much lower cost than more drilling. When petroleum prospecting moves offshore, the cost of seismology goes down by an order of magnitude, while the cost of drilling goes up by an order of magnitude.

Interested readers can purchase three volumes of reflection seismic images of the earth from the American Association of Petroleum Geologists (Bally [1983]).

Reproducibility of the Data

Reflection seismic data is voluminous. It is not like pencil marks on a sheet of paper. It is row upon row of high density magnetic tapes. Much seismic data is readily comprehensible. But much remains that is not, especially on the first try. Although

much data is incomprehensible and seems noisy and random, it is remarkable that the data is experimentally repeatable. And we find that by working with this data we learn more and more, and are encouraged to continue. Because there is so much still hidden in the data which is routinely collected, this book concentrates on the mainstream data geometry: single survey lines with conventional near-surface sources and receivers. Experimental techniques are indicated but not examined.

Computers as Imaging Devices

Philosophers ask the question, "What is knowledge?" As technologists, our answer is that there is a real world and there is also an image of it in our minds. Knowledge means that the two are similar. To help form images we use imaging devices, such as microscopes, telescopes, cameras, television, etc. In this book, computers are imaging devices for seismic echo soundings.

As an imaging device, a computer is in many ways ideal. A telescope is limited by the quality of its components. The image created by a computer is limited more by our understanding of mathematics, physics, and statistics than by limitations inherent in the computer. For imaging radar or ultrasonics, computer capacity would be a real problem. It happens that the information content (bandwidth) of seismic echo soundings is about matched by today's computers.

Why is it Fun?

Many young people seem to enjoy tackling tough theoretical problems, but when the time comes for application they are often disappointed to find that the theory is in some ways irrelevant or inadequate to the problem at hand. At first this causes a diminished interest in practical problems. But eventually many come to see the real problems as more interesting than the original mathematical models. Why is this?

Maybe life is like a computer game. I have noticed that the games students like best are not those with a predetermined, intricate logical structure. They like the games that allow them to gradually uncover the rules as they play. It is really fun when a period of frustration with a game is ended by some application of a personal idea. But to be fun, a game must *have* rules, and you must *be able* to uncover them with a reasonable amount of effort. Luckily, reflection seismology, together with modern computers, provides us with a similar environment. Sometimes a game can be too frustrating, and you need a hint to get you over some obstacle into a new and deeper level. Reading this book is not like playing the game. It is more like being given a collection of hints, a bag of tricks, to help you to the deeper level.

These tricks are mostly new, many being less than ten years old. They have been selected because they really work, not always, but often enough. I have repressed the urge to include many promising tricks that have not been sufficiently tested.

Practical problems are not only deeper than theoretical problems, but ultimately

they yield more interesting theory. For example, in freshman physics laboratory I learned to deduce Newton's laws of motion from simple experiments. I should have found experimentally that force equals mass times acceleration. Of course I didn't find exactly that. The experiment didn't seem to work out too well because of friction. *Friction,* now there's a really interesting subject for you. Physicists, chemists, metallurgists, earth scientists, they all know Newton's laws but wish they understood friction!

The theoretical book you are now holding wouldn't have been written except that two earlier theoretical approaches, (1) the theory of mathematical physics in stratified media and (2) time series analysis couldn't touch some of the most interesting aspects of our data. Some people thought we just had dirty data! Reflection seismic data are repeatable. Most of our problems really arise from the theory, not the data.

Computers and Movies

This book includes a number of computer programs. These programs are used for illustration and as exercises, but they should also be useful for reference. While they cannot be guaranteed, they worked for me when I generated many of the figures in this book, and they should work for you. You will notice that they are in a language similar to Fortran. The language is described in an appendix. Since everyone has different facilities for graphical output, to use these programs yourself, you will have to understand them well enough to direct their outputs into your plotting equipment.

A movie is really a stack of pictures. In a computer it is just a three-dimensional matrix of floating point numbers that must somehow be converted to brightness *pixels* (*pic*ture *el*ements). At the time of writing, few people are equipped to directly convert such a three-dimensional matrix into a movie. In our laboratory (Ottolini et al. [1984]) this is done on a high-quality video computer terminal (AED 512). Movie capability is a valuable asset. It enhances our understanding of our data and of the processing. Students are inspired by seeing their programming work result immediately in a movie, which is easily videotaped. Compared to other graphical devices this one is easy to maintain. It is used by both research students and students in the master's degree program, who use it for homework exercises.

The cost of such equipment, including the direct memory access (DMA) computer interface, is less than $10,000. For a really good experience with movies, you should also have physical control of a computer with a memory greater than a few megabytes. If you don't already have this, the price (1985) increases by about a factor of ten.

Will There Be Jobs ?

The main use of reflection seismic imaging is petroleum prospecting. Unlike nuclear energy, hydrocarbons are a nonrenewable resource and there is evidence that petroleum production must decline during the lifetimes of the young generation. Does

this mean that young people should avoid these studies? I think not. Taking the long-range view, with the population of the earth continuing to increase, it is not easy to imagine people losing interest in the earth's crust. A view of more intermediate range is that as the resource declines in abundance, there will be greater efforts to seek it. A short-range view is that workers are needed today, and there are no coal- or nuclear-powered airplanes. In any case, the skills developed in this book, computer implementations of concepts from physics, will always be of general utility.

Chapter 1

Introduction to imaging

1.1 EXPLODING REFLECTORS

The basic equipment for reflection seismic prospecting is a source for impulsive sound waves, a geophone (something like a microphone), and a multichannel waveform display system. A survey line is defined along the earth's surface. It could be the path for a ship, in which case the receiver is called a hydrophone. About every 25 meters the source is activated, and the echoes are recorded nearby. The sound source and receiver have almost no directional tuning capability because the frequencies that penetrate the earth have wavelengths longer than the ship. Consequently, echoes can arrive from several directions at the same time. It is the joint task of geophysicists and geologists to interpret the results. Geophysicists assume the quantitative, physical, and statistical tasks. Their main goals, and the goal to which this book is mainly directed, is to make good pictures of the earth's interior from the echoes.

1.1.1 A powerful analogy

Figure 1.1 shows two wave-propagation situations. The first is realistic field sounding. The second is a thought experiment in which the reflectors in the earth suddenly explode. Waves from the hypothetical explosion propagate up to the earth's surface where they are observed by a hypothetical string of geophones.

Notice in the figure that the ray paths in the field-recording case seem to be the same as those in the exploding-reflector case. It is a great conceptual advantage to imagine that the two wavefields, the observed and the hypothetical, are indeed the same. If they are the same, the many thousands of experiments that have really been done can be ignored, and attention can be focused on the one hypothetical experiment. One obvious difference between the two cases is that in the field geometry waves must first go down and then return upward along the same path, whereas in the hypothetical experiment they just go up. Travel time in field experiments could be divided by two. In practice, the data of the field experiments (two-way time) is analyzed assuming the sound velocity to be half its true value.

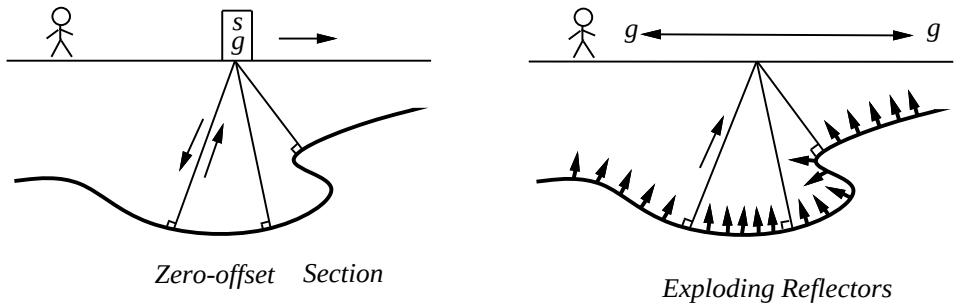

Figure 1.1: Echoes collected with a source-receiver pair moved to all points on the earth's surface (left) and the "exploding-reflectors" conceptual model (right). xrf-expref [NR]

1.1.2 Huygens secondary point source

Waves on the ocean have wavelengths comparable to those of waves in seismic prospecting (15-500 meters), but ocean waves move slowly enough to be seen. Imagine a long harbor barrier parallel to the beach with a small entrance in the barrier for the passage of ships. This is shown in Figure 1.2. A plane wave incident on the barrier from the open ocean will send a wave through the gap in the barrier. It is an observed fact that the wavefront in the harbor becomes a circle with the gap as its center. The difference between this beam of water waves and a light beam through a window is in the ratio of wavelength to hole size.

Linearity is a property of all low-amplitude waves (not those foamy, breaking waves near the shore). This means that two gaps in the harbor barrier make two semicircular wavefronts. Where the circles cross, the wave heights combine by simple linear addition. It is interesting to think of a barrier with many holes. In the limiting case of very many holes, the barrier disappears, being nothing but one gap alongside another. Semicircular wavefronts combine to make only the incident plane wave. Hyperbolas do the same. Figure 1.3 shows hyperbolas increasing in density from left to right. All those waves at nonvertical angles must somehow combine with one another to extinguish all evidence of anything but the plane wave.

A Cartesian coordinate system has been superimposed on the ocean surface with x going along the beach and z measuring the distance from shore. For the analogy with reflection seismology, people are confined to the beach (the earth's surface) where they make measurements of wave height as a function of x and t. From this data they can make inferences about the existence of gaps in the barrier out in the (x, z)-plane. Figure 1.4a shows the arrival time at the beach of a wave from the ocean through a gap. The earliest arrival occurs nearest the gap. What mathematical expression determines the shape of the arrival curve seen in the (x, t)-plane?

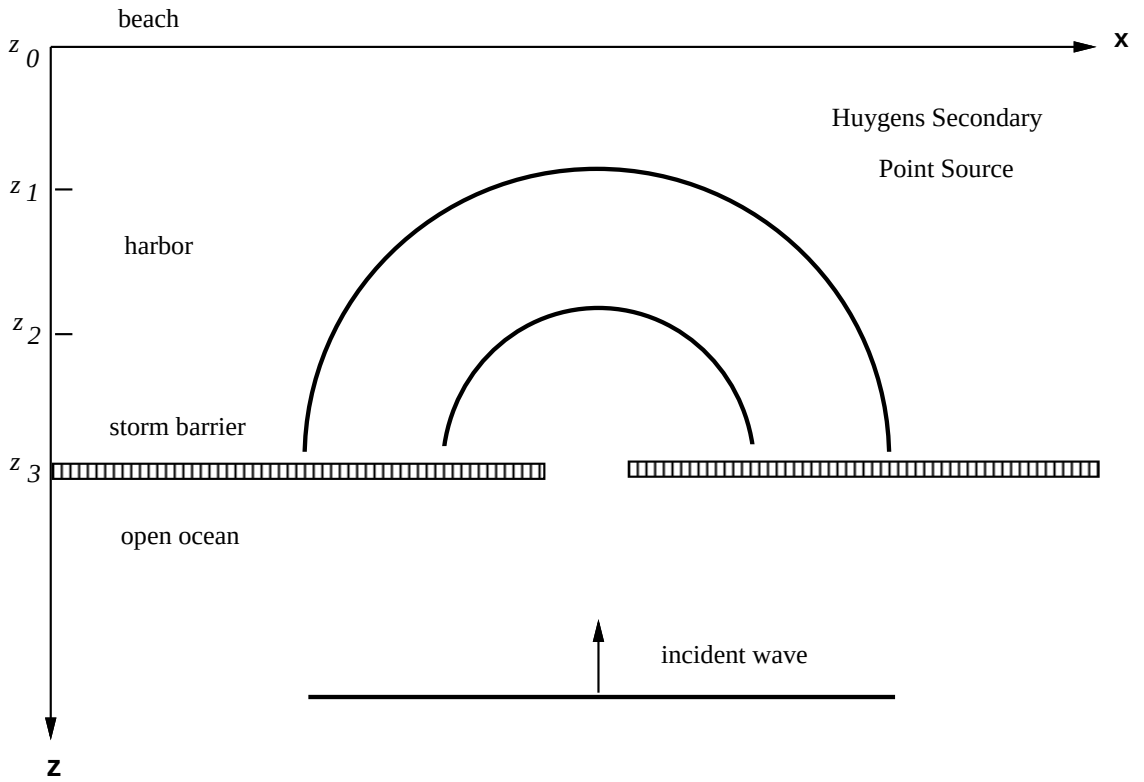

Figure 1.2: Waves going through a gap in a barrier have semicircular wavefronts (if the wavelength is long compared to the gap size). xrf-storm [NR]

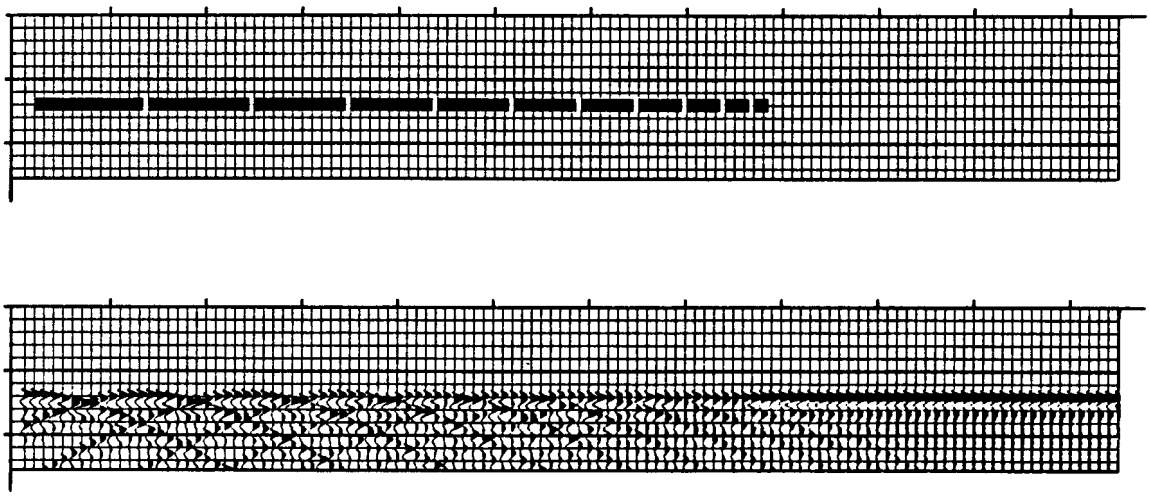

Figure 1.3: A barrier with many holes (top). Waves, (x, t)-space, seen beyond the barrier (bottom). xrf-storm2 [NR]

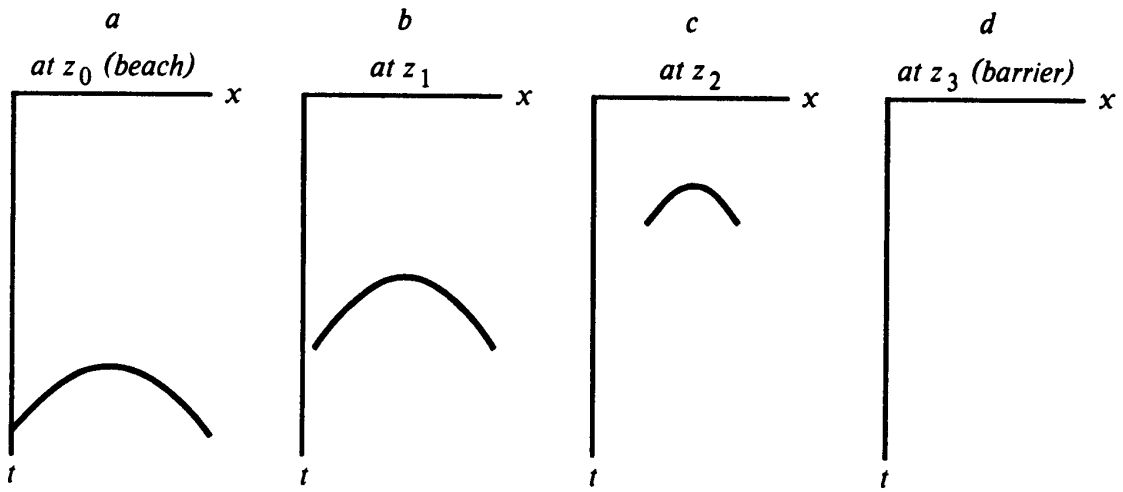

Figure 1.4: The left frame shows the hyperbolic wave arrival time seen at the beach. Frames to the right show arrivals at increasing distances out in the water. The x-axis is compressed from Figure 1.2. (Gonzalez) xrf-dc [NR]

The waves are expanding circles. An equation for a circle expanding with velocity v about a point (x_3, z_3) is

$$(x - x_3)^2 \;+\; (z - z_3)^2 \;=\; v^2 t^2 \tag{1.1}$$

Considering t to be a constant, i.e. taking a snapshot, equation (1.1) is that of a circle. Considering z to be a constant, it is an equation in the (x, t)-plane for a hyperbola. Considered in the (t, x, z)-volume, equation (1.1) is that of a cone. Slices at various values of t show circles of various sizes. Slices of various values of z show various hyperbolas. Figure 1.4 shows four hyperbolas. The first is the observation made at the beach $z_0 = 0$. The second is a hypothetical set of observations at some distance z_1 out in the water. The third set of observations is at z_2, an even greater distance from the beach. The fourth set of observations is at z_3, nearly all the way out to the barrier, where the hyperbola has degenerated to a point. All these hyperbolas are from a family of hyperbolas, each with the same asymptote. The asymptote refers to a wave that turns nearly 90° at the gap and is found moving nearly parallel to the shore at the speed dx/dt of a water wave. (For this water wave analogy it is presumed—incorrectly—that the speed of water waves is a constant independent of water depth).

If the original incident wave was a positive pulse, the Huygens secondary source must consist of both positive and negative polarities to enable the destructive interference of all but the plane wave. So the Huygens waveform has a phase shift. In the next section, mathematical expressions will be found for the Huygens secondary source. Another phenomenon, well known to boaters, is that the largest amplitude of the Huygens semicircle is in the direction pointing straight toward shore. The amplitude drops to zero for waves moving parallel to the shore. In optics this amplitude

drop-off with angle is called the *obliquity factor.*

1.1.3 Migration defined

A dictionary gives many definitions for the word *run.* They are related, but they are distinct. Similarly, the word *migration* in geophysical prospecting has about four related but distinct meanings. The simplest is like the meaning of the word *move.* When an object at some location in the (x, z)-plane is found at a different location at a later time t, then we say it *moves.* Analogously, when a wave arrival (often called an *event*) at some location in the (x, t)-space of geophysical observations is found at a different position for a different survey line at a greater depth z, then we say it *migrates.*

To see this more clearly, imagine the four frames of Figure 1.4 being taken from a movie. During the movie, the depth z changes beginning at the beach (the earth's surface) and going out to the storm barrier. The frames are superimposed in Figure 1.5a. Mainly what happens in the movie is that the event migrates upward

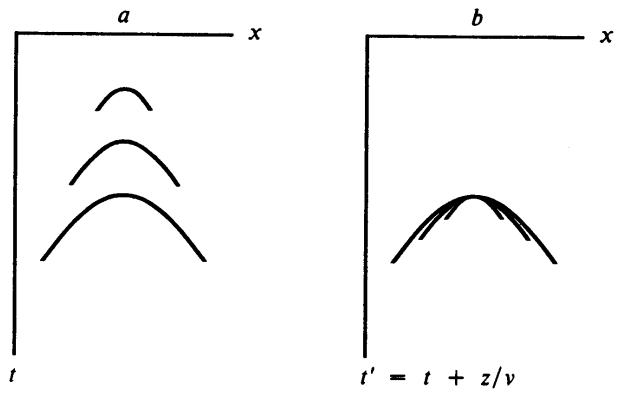

Figure 1.5: Left shows a superposition of the hyperbolas of Figure 1.4. At the right the superposition incorporates a shift, called retardation $t' = t + z/v$, to keep the hyperbola tops together. (Gonzalez) xrf-dcretard [NR]

toward $t = 0$. To remove this dominating effect of vertical translation make another superposition, keeping the hyperbola tops all in the same place. Mathematically, the time t axis is replaced by a so-called *retarded* time axis $t' = t + z/v$, shown in Figure 1.5b. The second, more precise definition of *migration* is the motion of an event in (x, t')-space as z changes. After removing the vertical shift, the residual motion is mainly a shape change. By this definition, hyperbola tops, or horizontal layers, do not migrate.

The hyperbolas in Figure 1.5 really extend to infinity, but the drawing cuts each one off at a time equal $\sqrt{2}$ times its earliest arrival. Thus the hyperbolas shown depict only rays moving within 45° of the vertical. It is good to remember this, that the ratio of first arrival time on a hyperbola to any other arrival time gives the cosine of the angle of propagation. The cutoff on each hyperbola is a ray at 45°. Notice that the end points of the hyperbolas on the drawing can be connected by a straight line. Also, the slope at the end of each hyperbola is the same. In physical space, the

angle of any ray is $\tan\theta = dx/dz$. For any seismic event, the slope $v\,dt/dx$ is $\sin\theta$, as you can see by considering a wavefront intercepting the earth's surface at angle θ. So, energy moving on a straight line in physical (x,z)-space migrates along a straight line in data (x,t)-space. As z increases, the energy of all angles comes together to a focus. The focus is the exploding reflector. It is the gap in the barrier. This third definition of migration is that it is the process that somehow pushes observational data—wave height as a function of x and t —from the beach to the barrier. The third definition stresses not so much the motion itself, but the transformation from the beginning point to the ending point.

To go further, a more general example is needed than the storm barrier example. The barrier example is confined to making Huygens sources only at some particular z. Sources are needed at other depths as well. Then, given a wave-extrapolation process to move data to increasing z values, exploding-reflector images are constructed with

$$\text{Image}\ (x,z) \quad = \quad \text{Wave}\ (t=0,x,z) \tag{1.2}$$

The fourth definition of migration also incorporates the definition of *diffraction* as the opposite of migration.

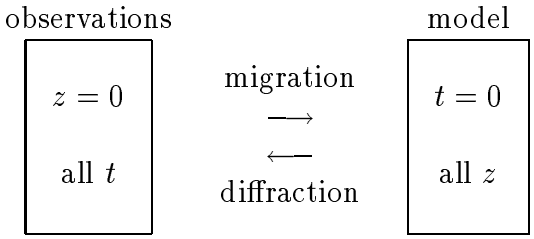

Diffraction is sometimes regarded as the natural process that creates and enlarges hyperboloids. *Migration* is the computer process that does the reverse.

Another aspect of the use of the word *migration* arises in chapter 6, where the horizontal coordinate can be either shot-to-geophone midpoint y, or offset h. Hyperboloids can be downward continued in both the (y,t)- and the (h,t)-plane. In the (y,t)-plane this is called *migration* or *imaging,* and in the (h,t)-plane it is called *focusing* or *velocity analysis.*

1.1.4 An impulse in the data

The Huygens diffraction takes an isolated pulse function (delta function) in (x,z)-space and makes it into a hyperbola in (x,t)-space at $z = 0$. The converse is to start from a delta function in (x,t)-space at $z = 0$. This converse refers to a seismic survey in which no echoes are recorded except at one particular location, and at that location only one echo is recorded. What earth model is consistent with such observations? As shown in Figure 1.6 this earth must contain a spherical mirror whose center is at the anomalous recording position.

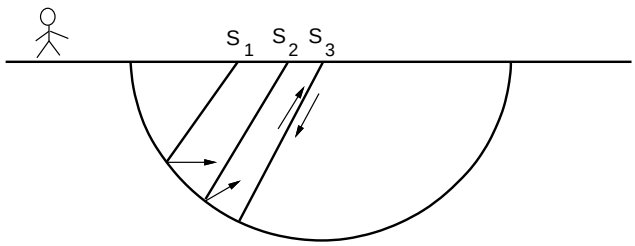

Figure 1.6: When the seismic source S is at the exact center of a semicircular mirror, then, and only then, will an echo return to the geophone at the source. This semicircular reflector is the logical consequence of a dataset where one echo is found at only one place on the earth. xrf-semicirc [NR]

It is unlikely that the processes of nature have created many spherical mirrors inside the earth. But when we look at migrated geophysical data, we often see spherical mirrors. Obviously, such input data contains impulses that are not consistent with the wave-propagation theory being explained here. This illustrates why petroleum prospectors study reflection seismic data processing, even though they personally plan to write no processing programs. The raw data is too complex to comprehend. The processed data gives an earth model, but its reliability is difficult to know. You may never plan to build an automobile, but when you drive alone far out into the desert, you should know as much as you can about automobiles.

1.1.5 Hand migration

Given a seismic event at (x_0, t_0) with a slope $p = dt/dx$, let us determine its position (x_m, t_m) after migration. Consider a planar wavefront at angle θ to the earth's surface traveling a distance dx in a time dt. Assuming a velocity v we have the wave angle in terms of measurable quantities.

$$\sin\,\theta \quad = \quad \frac{v\;dt}{dx} \quad = \quad p\,v \tag{1.3}$$

The vertical travel path is less than the angled path by

$$t_m \quad = \quad t_0\,\cos\,\theta \quad = \quad t_0\,\sqrt{1\;-\;p^2\,v^2} \tag{1.4}$$

A travel time t_0 and a horizontal component of velocity $v\,\sin\,\theta$ gives the lateral location after migration:

$$x_m \quad = \quad x_0\;-\;t_0\,v\,\sin\,\theta \quad = \quad x_0\;-\;t_0\,p\,v^2 \tag{1.5}$$

Consideration of a hyperbola migrating towards its apex shows why (1.5) contains a minus sign. Equations (1.4) and (1.5) are the basic equations for manual migration of reflection seismic data. They tell you where the point migrates, but they do not tell you how the slope p will change.

1.1.6 Reflector steepening

Consider a vertical wall, a limiting case of a dipping bed. Its reflections, the asymptotes of a hyperbola, have a nonvertical steepness. This establishes that migration increases the apparent steepness of dipping beds. I use the words *apparent steepness* because it is the slope as seen in the (x, t)-plane that has steepened. Migration really produces its output in z, but z/v is often overlain on t to create a *migrated time section*. When we say a hyperbola migrates to its apex, we are of course thinking of the migrated time section. Let us determine the steepening as a function of angle.

Consider a point $(x_{0+}, t_{0+}) = (x_0 + \Delta,\ t_0 + p\Delta)$ neighboring the original point (x_0, t_0). By equations (1.4) and (1.5), this neighbor migrates to

$$t_{m+} = (t_0 + p\,\Delta)\,\sqrt{1 - p^2\,v^2} \tag{1.6}$$

$$x_{m+} = x_0 + \Delta - (t_0 + p\,\Delta)\,p\,v^2 \tag{1.7}$$

Now we compute the stepout p_m of the migrated event

$$p_m = \frac{dt_{m+}}{dx_{m+}} = \frac{dt_{m+}/d\Delta}{dx_{m+}/d\Delta}$$

$$p_m = \frac{p\,\sqrt{1 - p^2\,v^2}}{1 - p^2\,v^2} = \frac{p}{\sqrt{1 - p^2\,v^2}} = \frac{\tan\,\theta}{v} \tag{1.8}$$

So slopes on migrated time sections, like slopes in Cartesian space, imply tangents of angles while slopes on unmigrated time sections imply sines.

It may seem paradoxical that dipping beds change slope on migration whereas flanks of hyperbolas do not change slope during downward continuation. One reason is that migration is downward continuation *plus* imaging (selecting $t = 0$). Another reason is that a hyperbola is a special event that comes from a single source at a single depth whereas a dipping bed is a superposition of point sources from different depths. Figure 1.7 shows how points making up a line reflector diffract to a line reflection, and how points making up a line reflection migrate to a line reflector.

1.1.7 Limitations of the exploding-reflector concept

The exploding-reflector concept is a powerful and fortunate analogy. For people who spend their time working entirely on data interpretation rather than on processing, the exploding-reflector concept is more than a vital crutch. It's the only means of transportation! But for those of us who work on data processing, the exploding-reflector concept has a serious shortcoming. No one has yet figured out how to extend the concept to apply to data recorded at nonzero offset. Furthermore, most data is recorded at rather large offsets. In a modern marine prospecting survey, there is not one hydrophone, but hundreds, which are strung out in a cable towed behind the ship. The recording cable is typically 2-3 kilometers long. Drilling may be about 3

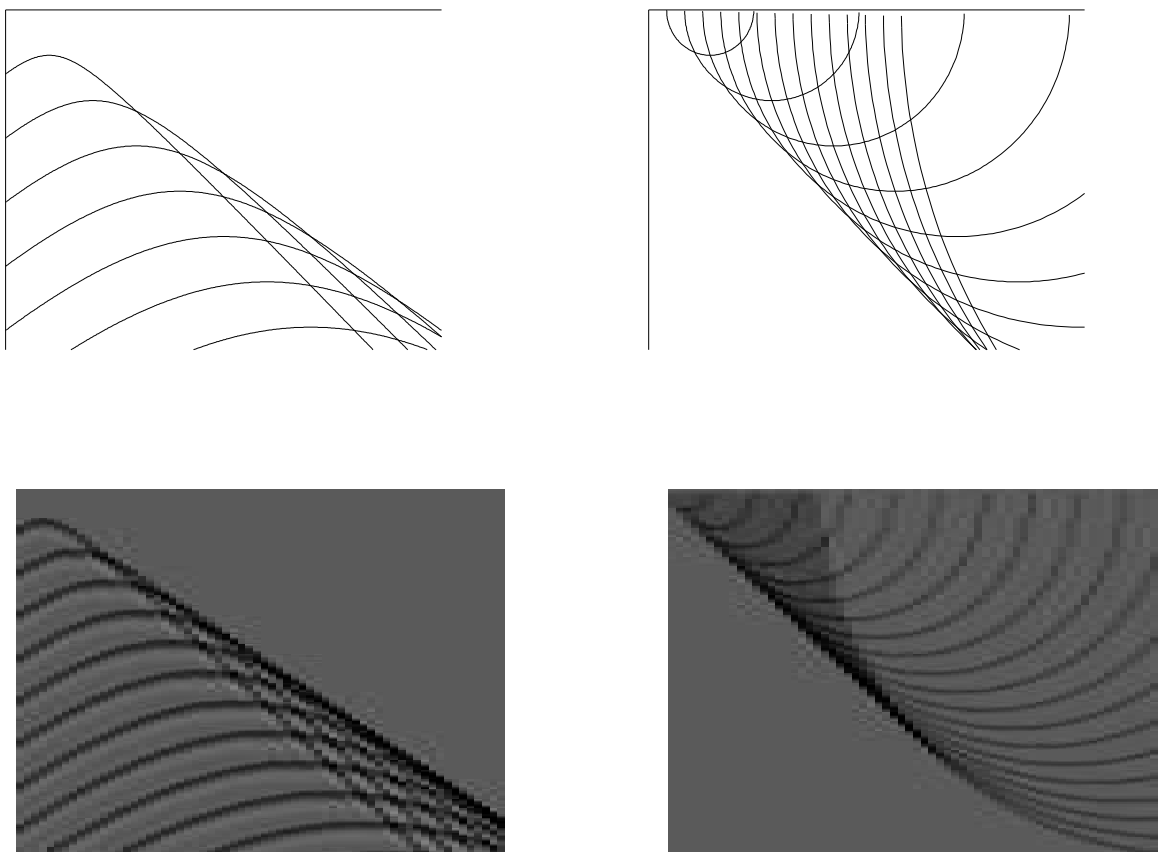

Figure 1.7: Left is a superposition of many hyperbolas. The top of each hyperbola lies along a straight line. That line is like a reflector, but instead of using a continuous line, it is a sequence of points. Constructive interference gives an apparent reflection off to the side. Right shows a superposition of semicircles. The bottom of each semicircle lies along a line that could be the line of an observed plane wave. Instead the plane wave is broken into point arrivals, each being interpreted as coming from a semicircular mirror. Adding the mirrors yields a more steeply dipping reflector. xrf-dip [ER]

kilometers deep. So in practice the angles are big. Therein lie both new problems and new opportunities, none of which will be considered until chapter 6.

Furthermore, even at zero offset, the exploding-reflector concept is not quantitatively correct. For the moment, note three obvious failings: First, Figure 1.8 shows rays that are not predicted by the exploding-reflector model. These rays will be

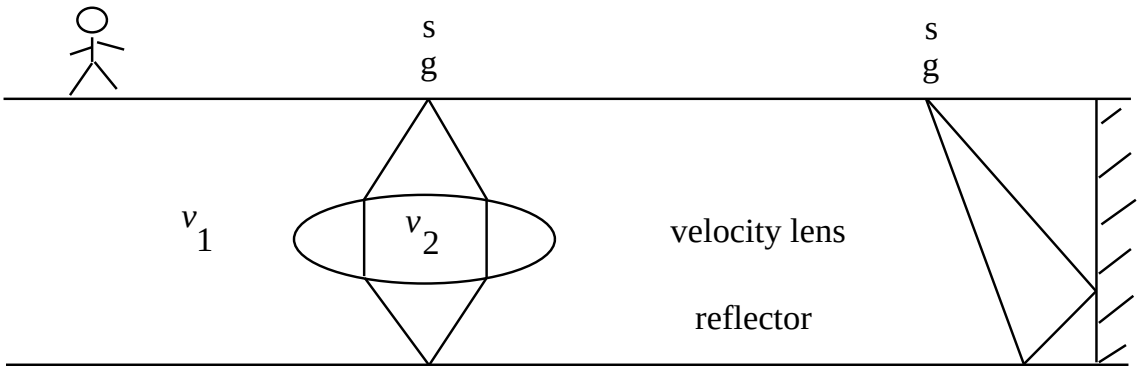

Figure 1.8: Two rays, not predicted by the exploding-reflector model, that would nevertheless be found on a zero-offset section. xrf-fail [NR]

present in a zero-offset section. Lateral velocity variation is required for this situation to exist.

Second, the exploding-reflector concept fails with multiple reflections. For a flat sea floor with a two-way travel time t_1, multiple reflections are predicted at times $2t_1$, $3t_1$, $4t_1$, etc. In the exploding-reflector geometry the first multiple goes from reflector to surface, then from surface to reflector, then from reflector to surface, for a total time $3t_1$. Subsequent multiples occur at times $5t_1$, $7t_1$, etc. Clearly the multiple reflections generated on the zero-offset section differ from those of the exploding-reflector model.

The third failing of the exploding-reflector model is where we are able to see waves bounced from both sides of an interface. The exploding-reflector model predicts the waves emitted by both sides have the same polarity. The physics of reflection coefficients says reflections from opposite sides have opposite polarities.

1.1.8 Plate tectonics example

Plate tectonic theory says the ocean floors are made of thin plates that are formed at volcanic ridges near the middle of the oceans. These plates move toward trenches in the deepest part of the ocean where they plunge back down into the earth. The best evidence for the theory is the lack of old rocks on the floors of the earth's oceans. Generally, continents are older rocks jostled by the younger moving oceanic plates. The formation of plates by mid-ocean ridge volcanism is readily observed in a variety of ways. Whether the plates really do plunge at the trenches is not so clear observationally. The evidence comes from earthquake locations and from reflection seismology. Figure 1.9 shows some reflection data from the Japan trench. Two reflections dominate, the sea floor reflection and a deeper layer dipping down to the

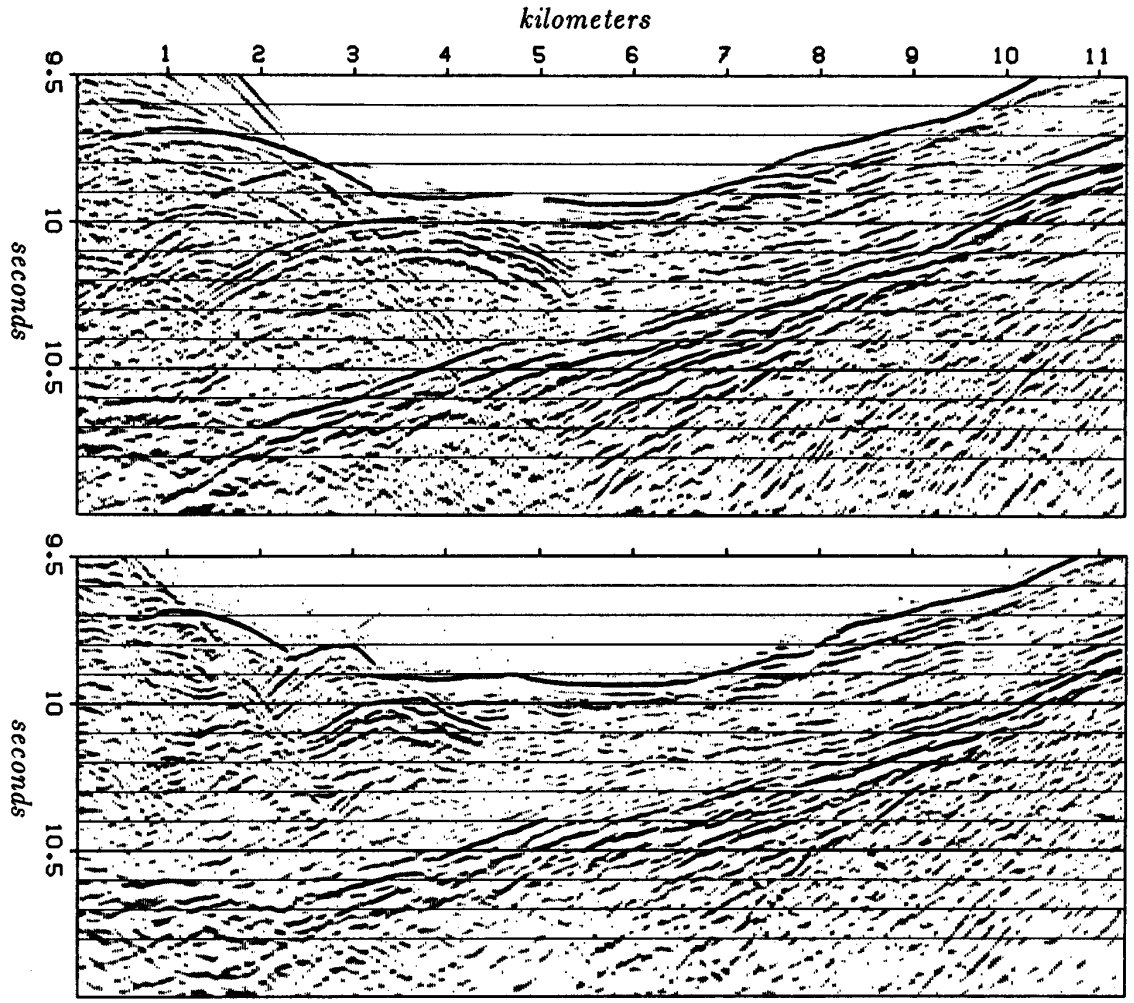

Figure 1.9: Top is 11 kilometers of reflection data from a survey line across the Japan trench (Tokyo University Oceanographic Research Institute). Bottom shows the result of migration processing. (Ottolini) xrf-japan [NR]

left. This latter is presumably the top part of a plate that is beginning its descent into the earth. We can examine it for evidence of bending downward, such as tension fractures near the surface. (The topmost layer is soft recent marine sediment loosely attached to the plate). Notice that the top of the plot is not zero time. The time axis runs from 9.5 to 11.0 seconds. Before 9.5 sec there are no echoes—we are waiting for the waves to go between the ship and the ocean floor. Hyperbolic reflections around kilometers 1-3 are collapsed by migration to form interesting "blocky" shapes. Look at the sea floor topography near kilometer 8 and the difference between migrated and unmigrated data sections. After migration, the sea floor diffraction hyperbolas move away from the plate echo (kilometer 4). Fractures (especially the one at 6.2 km) are more sharply defined. Finally, if the plate bends downward, it is not apparent from the data given. The bending question really requires a more detailed analysis of lateral variation in seismic velocity.

For an example with petroleum interest, see Figure 1.10, data from offshore Texas. Sediments are dropped where coastal rivers enter the Gulf of Mexico. The added

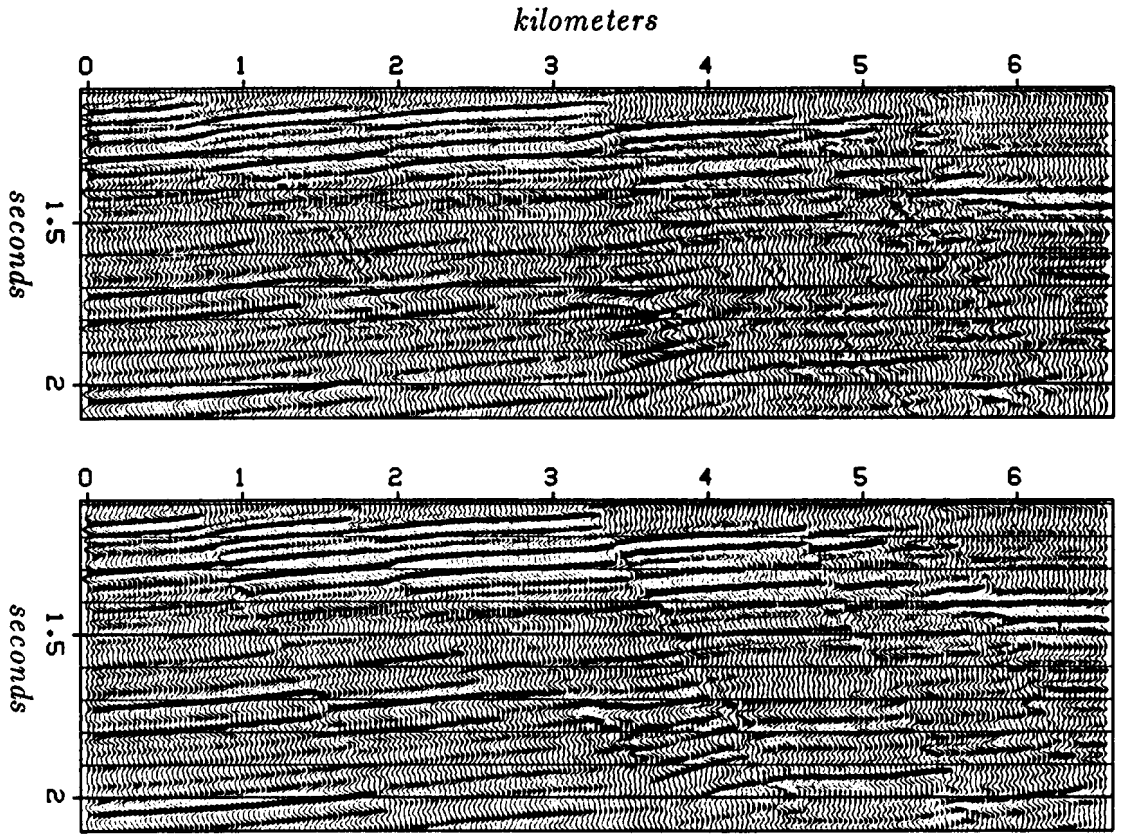

Figure 1.10: Top is 6.5 kilometers of reflection data from a survey line offshore from the Texas coast of the Gulf of Mexico. Bottom shows the result of migration processing. (Rothman). xrf-growth [NR]

weight causes slumping along steep faults. After a permeable sandstone layer has been identified by drilling, its reflection can be extrapolated up dip to the nearest fault on

data like Figure 1.10. The fault is likely to break the continuity of the permeability trapping the upward flowing hydrocarbons. A sandstone at this depth can have a porosity of 25%. Assume a seismic velocity of 2.2 km/sec. Deduce the scale between physical volume and the data in Figure 1.10. Comparing the value of a volume of oil to the size of that same volume on Figure 1.10, you can see the importance of good images.

EXERCISES:

1 Prove the Pythagorean theorem, that is, the length of the hypotenuse $v\,t$ of a right triangle is determined by $x^2 + z^2 = v^2 t^2$. Hint:

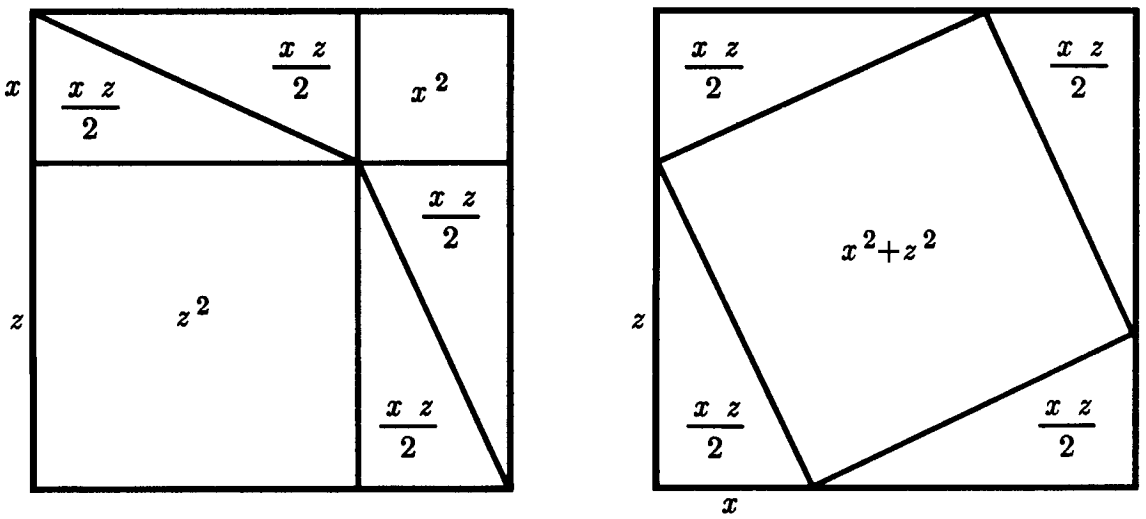

Figure 1.11: xrf-pythag [NR]

2 Compute propagation angles for the hyperbola flanks in Figure 1.9.

3 Using the result of exercise 2, deduce the plunge angle of the plate.

4 How deep is the Japan trench (water velocity is 1.5 km/sec)?

5 On the Gulf Coast data, which direction is offshore? Why?

1.2 SURROUNDING DISCIPLINES

The previous section considered the *geometrical* aspects of wave propagation and how they relate to seismic imaging. Here we consider all the surrounding disciplines, how they relate, how they fail to relate to our central topic of earth imaging. Physics, the kind of physics one learns as an undergraduate, has a relevance to earth imaging, and also an irrelevance—the simple models don't always work. Likewise, mathematics, with its precise problem formulations is both relevant, and irrelevant to earth imaging.

And geophysics itself, with its classic areas of theory and observation is both relevant and irrelevant to practical earth imaging. Finally geology brings insights as to why and why not basic physics is a realistic guide to practice. In all the surrounding disciplines of physics, mathematics, geophysics, and geology, I will give you some indication of the degree to which theory can be used as a guide by pointing out some inconsistencies between theory and current industrial practice.

1.2.1 Physics

Derivation of the acoustic wave equation

The acoustic wave equation describes sound waves in a liquid or gas. Another more complicated set of equations describes elastic waves in solids. Begin with the acoustic case. Define

ρ = mass per unit volume of the fluid
u = velocity flow of fluid in the x-direction
w = velocity flow of fluid in the z-direction
P = pressure in the fluid

Newton's law of momentum conservation says that a small volume within a gas will accelerate if there is an applied force. The force arises from pressure differences at opposite sides of the small volume. Newton's law says

$$\text{mass} \times \text{acceleration} = \text{force} = -\text{ pressure gradient}$$

$$\rho \frac{\partial u}{\partial t} = -\frac{\partial P}{\partial x} \tag{1.9}$$

$$\rho \frac{\partial w}{\partial t} = -\frac{\partial P}{\partial z} \tag{1.10}$$

The second physical process is energy storage by compression and volume change. If the velocity vector u at $x + \Delta x$ exceeds that at x, then the flow is said to be diverging. In other words, the small volume between x and $x + \Delta x$ is expanding. This expansion must lead to a pressure drop. The amount of the pressure drop is in proportion to a property of the fluid called its *incompressibility* K. In one dimension the equation is

$$\text{pressure drop} = (\text{incompressibility}) \times (\text{divergence of velocity}) \tag{1.11}$$

$$-\frac{\partial P}{\partial t} = K \frac{\partial u}{\partial x} \tag{1.12}$$

In two dimensions it is

$$-\frac{\partial P}{\partial t} = K \left(\frac{\partial u}{\partial x} + \frac{\partial w}{\partial z} \right) \tag{1.13}$$

To arrive at the one-dimensional wave equation from (1.9) and (1.12), first divide (1.9) by ρ and take its x-derivative:

$$\frac{\partial}{\partial x}\,\frac{\partial}{\partial t}\;u \;=\; -\,\frac{\partial}{\partial x}\,\frac{1}{\rho}\,\frac{\partial P}{\partial x} \tag{1.14}$$

Second, take the time-derivatives of (1.12) and (1.13). In the solid-earth sciences we are fortunate that the material in question does not change during our experiments. This means that K is a constant function of time:

$$\frac{\partial^2 P}{\partial t^2} \;=\; -\,K\,\frac{\partial}{\partial t}\,\frac{\partial}{\partial x}\,u \tag{1.15}$$

Inserting (1.14) into (1.15), the one-dimensional scalar wave equation appears.

$$\frac{\partial^2 P}{\partial t^2} \;=\; K\,\frac{\partial}{\partial x}\,\frac{1}{\rho}\,\frac{\partial P}{\partial x} \tag{1.16}$$

In two space dimensions, the exact, acoustic scalar wave equation is

$$\frac{\partial^2 P}{\partial t^2} \;=\; K\left(\frac{\partial}{\partial x}\,\frac{1}{\rho}\,\frac{\partial}{\partial x} \;+\; \frac{\partial}{\partial z}\,\frac{1}{\rho}\,\frac{\partial}{\partial z}\right) P \tag{1.17}$$

You will often see the scalar wave equation in a simplified form, in which it is assumed that ρ is not a function of x and z. Two reasons are often given for this approximation. First, observations are generally unable to determine density, so density may as well be taken as constant. Second, we will soon see that Fourier methods of solution do not work for space variable coefficients. Before examining the validity of this approximation, its consequences will be examined. It immediately reduces (1.17) to the usual form of the scalar wave equation:

$$\boxed{\frac{\partial^2 P}{\partial t^2} \;=\; \frac{K}{\rho}\left(\frac{\partial^2}{\partial x^2} \;+\; \frac{\partial^2}{\partial z^2}\right) P} \tag{1.18}$$

To see that this equation is a restatement of the geometrical concepts of previous sections, insert the trial solution

$$P \;=\; \exp(-\,i\omega t \;+\; i\,k_x x \;+\; i\,k_z z) \tag{1.19}$$

What is obtained is the *dispersion relation of the two-dimensional scalar wave equation:*

$$\frac{\omega^2}{K/\rho} \;=\; k_x^2 \;+\; k_z^2 \tag{1.20}$$

Later an equation like (1.20) will be developed by considering only the geometrical behavior of waves. In that development the wave velocity squared is found where

K/ρ stands in equation (1.20). Thus physics and geometry will be reconciled by the association

$$v^2 \quad = \quad \frac{K}{\rho} \tag{1.21}$$

Last, let us see why Fourier methods fail when the velocity is space variable. Assume that ω, k_x, and k_z are constant functions of space. Substitute (1.19) into (1.18) and you get the contradiction that ω, k_x, and k_z must be space variable if the velocity is space variable. Try again assuming space variability, and the resulting equation is still a differential equation, not an algebraic equation like (1.20).

Reflections and the high-frequency limit

It is well known that the contact between two different materials can cause acoustic reflections. A material contact is defined to be a place where either K or ρ changes by a spatial step function. In one dimension either $\partial K/\partial x$ or $\partial \rho/\partial x$ or both would be infinite at a point, and we know that either can cause a reflection. So it is perhaps a little surprising that while the density derivative is explicitly found in (1.17), the incompressibility derivative is not. This means that dropping the density gradients in (1.17) will not eliminate all possible reflections. Dropping the terms will slightly simplify further analysis, however, and since constant density is a reasonable case, the terms are often dropped.

There are also some well-known mathematical circumstances under which the first-order terms may be ignored. Fix your attention on a wave going in any particular direction. Then ω, k_x, and k_z have some prescribed ratio. In the limiting case that frequency goes to infinity, the P_{tt}, P_{xx}, and P_{zz} terms in (1.18) all tend to the *second* power of infinity. Suppose two media gradually blend into one another so that $\partial \rho/\partial x$ is less than infinity. The terms neglected in going from (1.17) to (1.18) are of the form $\rho_x P_x$ and $\rho_z P_z$. As frequency tends to infinity, these terms only tend to the *first* power of infinity. Thus, in that limit they can be neglected.

These terms are usually included in theoretical seismology where the goal is to calculate synthetic seismograms. But where the goal is to create earth models from seismic field data—as in this book—these terms are generally neglected. Earth imaging is more difficult than calculating synthetic seismograms. But often the reason for neglecting the terms is simply to reduce the clutter. These terms may be neglected for the same reason that equations are often written in two dimensions instead of three: the extension is usually possible but not often required. Further, these terms are often ignored to facilitate Fourier solution techniques. Practical situations might arise for which these terms need to be included. With the finite-difference method, they are not difficult to include. But any effort to include them in data processing should also take into account other factors of similar significance, such as the assumption that the acoustic equation approximates the elastic world.

EXERCISES:

1 Soil is typically saturated with water below a certain depth, which is known as the *water table.* Experience with hammer-seismograph systems shows that seismic velocity typically jumps up to water velocity ($V_{-2H_2O} = 1500\ m/s$) at the water table. Say that in a certain location, the ground roll is observed to be greater than the reflected waves, so a decision has been made to bury geophones. The troublesome ground roll is observed to travel at six-tenths the speed of a water wave. How deep must the geophones be buried below the water table to attenuate the ground roll by a factor of ten? Assume the data contains all frequencies from 10 to 100 Hz. (Hints: $\ln 10 \approx 2$, $2\pi \approx 6$, etc.)

2 Consider the function

$$P(z,t) \quad = \quad P_0 \, \frac{1}{\sqrt{Y(z)}} \, e^{\,i\omega\, t \,-\, i \int_0^z \, \omega \sqrt{\frac{\rho(\xi)}{K(\xi)}} \, d\xi} \tag{1.22}$$

where

$$\begin{aligned} P_0 \quad &= \quad \text{constant} \\ Y \quad &\equiv \quad \frac{1}{\sqrt{\rho(z)\, K(z)}} \end{aligned}$$

as a trial solution for the one-dimensional wave equation:

$$\left(\frac{\partial^2}{\partial t^2} \; - \; \frac{K(z)}{\rho(z)} \, \frac{\partial^2}{\partial z^2} \right) P \quad = \quad - \, \frac{K(z)}{\rho(z)^2} \, \frac{\partial \rho}{\partial z} \, \frac{\partial P}{\partial z} \tag{1.23}$$

Substitute the trial solution (1.22) into the wave equation (1.23). Discuss the trade-off between changes in material properties and the validity of your solution for different wavelengths.

Failure of Newtonian viscosity

Also remarkable is the failure of basic textbook seismology to explain the observed frequency-dependence of the dissipation parameter Q. The simplest theoretical approach to dissipation is to add a strain-rate term to Hooke's stress-strain law. This predicts stronger relative dissipation of high frequencies than of low frequencies. Experimentally, relative dissipation is observed to be roughly constant over many decades of frequency. Other simple Newtonian theories yield polynomial ratios in $-i\omega$ for the stress/strain ratio. These theories contain scale lengths and characteristic frequencies. They do not predict constant Q. The heterogeneity of the rock at all scales seems to be an essential attribute of a successful theory.

1.2.2 Geophysics

Curiously, our closest discipline, general geophysics, also seems to contradict, as well as support, some of the things we try to do in earth imaging.

Nonobservation of converted shear waves

In earthquake seismology and in laboratory measurement there are two clearly observed velocities. The faster velocity is a pressure wave (P-wave), and the slower velocity is a shear wave (S-wave). The shear wave can be polarized with ground motion in a horizontal plane (SH) or in a vertical plane (SV). Theory, field data, and laboratory measurement are in agreement. Successful experimental work with S-waves in the prospecting environment was done by Cherry and Waters [1968] and Erickson, Miller and Waters [1968].

It is remarkable that more than 99% of industrial petroleum prospecting ignores the existence of shear waves. Mathematically the earth is treated as if it were a liquid or a gas. The experimental work with shear waves used special equipment to generate and record vibration perpendicular to the survey line, i.e. SH-waves. The picture of the earth given by these transverse waves is often impaired by the soil layers, but sometimes the SH-wave picture is clear and consistent. Surprisingly, even good SH-wave data is often difficult to relate to the P-wave picture. These experimental studies show that the shear waves typically travel about half the speed of the pressure waves except in the soil layer, where the shear wave speed is often much slower and more variable. Observed shear waves usually have lower frequency than pressure waves. A shear wave with half the frequency and half the velocity of a pressure wave has just the same wavelength and hence the same resolving power as the pressure wave. Indeed, experimental work shows that shear waves do offer us about the same spatial resolution as pressure waves. Most land seismic data shows only the vertical component of motion, and all marine seismic data records the pressure. So in the conventional recording geometry, ideally we should never see SH-waves. More precisely, SH-waves should be small, arising only from the earth's departure from simple stratification.

The puzzling aspect of shear waves in reflection seismology is the failure of petroleum prospectors using the standard operating arrangement to routinely observe P-to-S conversions. Theory predicts that P-waves hitting an interface at an angle should be partially converted to SV-waves. Furthermore, for the 30°-60° angle reflections that are routinely encountered, these converted waves should have a size comparable to the P-wave.

The routine geometry of recording and processing discriminates somewhat against converted shear waves. But it discriminates against multiple reflections too (in much the same way) and we see multiples all the time. Furthermore the signature of converted waves should resemble that of multiples, but be distinctly different. Converted waves should show up routinely in velocity surveys (chapter 6). Figure 1.12 shows a zero-offset section containing some multiple reflections. The multiple reflection is recognizable as a replica of earlier topography. Converted waves would replicate the topography but the time scaling would be in the ratio of about 3/2 instead of exactly 4/2. With a sufficiently complex topography, as in Figure 1.12, the probability is low that the converted wave would be mistaken for another primary reflection.

Figure 1.12: A zero-offset section from east Africa with multiple reflections. (Teledyne) xrf-africa [NR]

Converted waves should have good diagnostic value in exploration. But the likelihood of seeing converted shear waves in conventional data seems to be so remote that most interpreters have given up looking. Why aren't converted waves seen in conventional data? Some reasons can be offered:

- In marine data there would have to be an additional conversion to P for the water path.
- In land data the soil is especially absorptive of shear.
- Vertical component recorders tend to see P better than S. This is especially so because rays bend toward the vertical in the near surface.

Of all the reasons why converted shear waves should be weaker than pressure waves, none is overwhelming. A wide range of amplitudes are recorded in a wide variety of environments. Data are often displayed with automatic gain control (AGC). Weakened amplitude appears to be insufficient cause for the failure of observation. We should keep looking. Converted waves are certainly more prevalent than our recognition of them. (I have never identified a converted shear wave on conventional recordings).

So although converted shear waves might some day play a significant role in reflection seismology, we now return to the mainstream—how to deal effectively with that which is routinely observable.

Reliability of reverberation modeling

The seismological literature contains an abundance of theory to describe seismic waves in layered media. A significant aspect of applied seismology is the general neglect of intrabed reverberation. When a wave reflects from an interface, the strength of the reflected wave is a small fraction, typically less than 10%, of the strength of the incident wave. This reflected wave is the one that is mainly dealt with in this book. However, the reflected wave itself reflects again and again, ad infinitum. For short path geometries, there can be very many of these rays. The question is whether these reverberations can ever amount to enough to make considering them worthwhile. The answer seems to be that although reverberation may be significant, seismologists are rarely able to improve interpretation of reflection survey data with the more complicated theory that is required to incorporate reverberation.

The situation is somewhat improved when well logs are available, but even then there are serious difficulties. The best possible lateral resolving power, say about 20-50 meters, is obtained after migration. The well log, however, is not a 20-50 meter lateral average of the earth. Next time you see a highway cut through sedimentary rocks, think of the difference between a point and a lateral average over 20-50 meters. In practice, people smooth the well log (vertical smoothing). Too little smoothing gives too much reverberation. Too much smoothing gives no reverberation. The amount of vertical smoothing is an empirically determined parameter, and results are significantly sensitive to it. Vertical averages of the well log may or may not be a satisfactory approximation to the required horizontal average.

What you can get from reflection seismology

Luckily, it has been discovered that certain functions of ρ and K can be reliably determined and mapped. The velocity v and the acoustic impedance R are given by the equations

$$v = \sqrt{K/\rho} \tag{1.24}$$

$$R = \sqrt{K\rho} \tag{1.25}$$

Mathematically, it is a simple job to back-solve equations (1.24) and (1.25), which gives

$$K = v\,R \tag{1.26}$$

$$\rho = \frac{R}{v} \tag{1.27}$$

In practice, the solutions (1.26) and (1.27) have little value because the two parameters v and R are seen through nonoverlapping spectral windows. The acoustic impedance R is seen through the typical 10 to 100 Hz spectral window of good quality reflection data. Since the low frequency part of the spectrum is missing, it is common

to say that it is not the impedance which is seen, but the gradient *reflectivity* $= c(x,z) = d\ln R/dz = R^{-1}dR/dz$ which is more familiar at a layer boundary where it has the form $(R_1 - R_2)/(R_1 + R_2)$.

The velocity v is seen through a much smaller window. Observation of it involves studying travel time as shot-to-geophone offset varies and will be described in chapter 6. With this second window it is hard to discern sixteen independent velocity measurements on a 4-second reflection time axis. So this window goes from zero to about 2 Hz, as depicted in Figure 1.13.

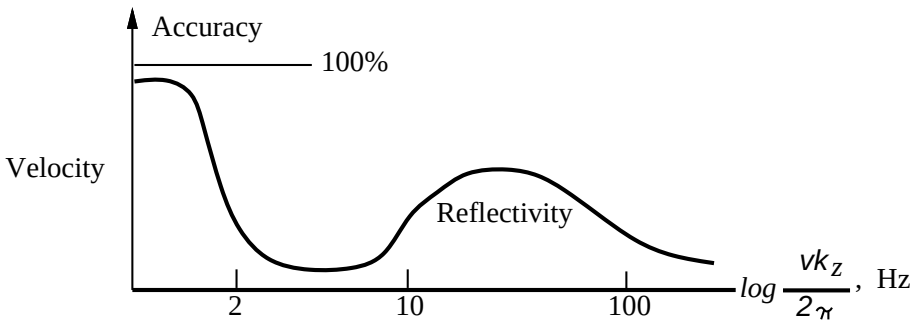

Figure 1.13: Reliability of information obtained from surface seismic measurements. xrf-rely [NR]

Note that there is an information gap from 2-10 Hz. Even presuming that *rock physics* can supply us with a relationship between ρ and K, the gap seriously interferes with the ability of a seismologist to predict a well log before the well is drilled. What seismologists can do somewhat reliably is predict a filtered log.

The observational situation described above has led reflection seismologists to a specialized use of the word *velocity.* To a reflection seismologist, *velocity* means the low spatial frequency part of "real velocity." The high-frequency part of the "real velocity" isn't called *velocity:* it is called *reflectivity.* Density is generally disregarded as being almost unmeasurable by surface reflection seismology.

1.2.3 Mathematics

Philosophy of inverse problems

Physical processes are often simulated with computers in much the same way they occur in nature. The machine memory is used as a map of physical space, and time evolves in the calculation as it does in the simulated world. A nice thing about solving problems this way is that there is never any question about the uniqueness of the solution. Errors of initial data and model discretization do not tend to have a catastrophic effect. Exploration geophysicists, however, rarely solve problems of this type. Instead of having (x,z)-space in the computer memory and letting t evolve, we usually have (x,t)-space in memory and extrapolate in depth z. This is our business,

taking information (data) at the earth's surface and attempting to extrapolate to information at depth. Stable time evolution in nature provides no "existence proof" that our extrapolation goals are reasonable, stable, or even possible.

The time-evolution problems are often called *forward problems* and the depth-extrapolation problems *inverse problems.* In a *forward problem,* such as one with acoustic waves, it is clear what you need and what you can get. You need the density $\rho(x,z)$ and the incompressibility $K(x,z)$, and you need to know the initial source of disturbance. You can get the wavefield everywhere at later times but you usually only want it at the earth's surface for comparison to some data. In the *inverse problem* you have the waves seen at the surface, the source specification, and you would like to determine the material properties $\rho(x,z)$ and $K(x,z)$. What has been learned from experience is that routine observations do not give reasonable estimates of images or maps of ρ and K.

Mathematical inverse problems

In mathematics the solution to an inverse problem has come to mean the "determination" of material properties from wavefields. Often this is achieved with a "convergent sequence." Geophysicists are less precise (or more inclusive) about what they mean by "determination." In some chapters of this book reflectors are "determined" by the exploding-reflection concept. In chapter 6 shot-to-geophone offset is incorporated, and reflectivity $c(x,z)$ and velocity $v(z)$ are "determined" with a buried-experiment concept. In chapter 11 the concept is developed of suppressing multiple reflections and finding the "true" amplitudes of reflections by having the upcoming wave vanish before the onset of the downgoing wave. Other imaging concepts seem likely to result from future processing schemes. It might be possible to show that some of our "determinations" coincide with those of mathematicians, but such coincidence is not our goal here. Such a goal is formulated more directly in my third book *Earth soundings analysis: processing versus inversion.*

1.2.4 Geology

Because of the complexity of sedimentary rocks, there is not universal agreement on an appropriate mathematical description.

The clastic section

Generally speaking, most petroleum reservoir rocks are sandstones. Sandstones are most often made by the sands that are deposited near the mouths of rivers where the water velocity is no longer sufficient to move them. The sands deposit along the terminus of the sand bars found at the river mouth, often along a slope of 25° or so, as depicted in Figure 1.14. Although the sands are not laid down in flat layers, the process may build a horizontal layer.

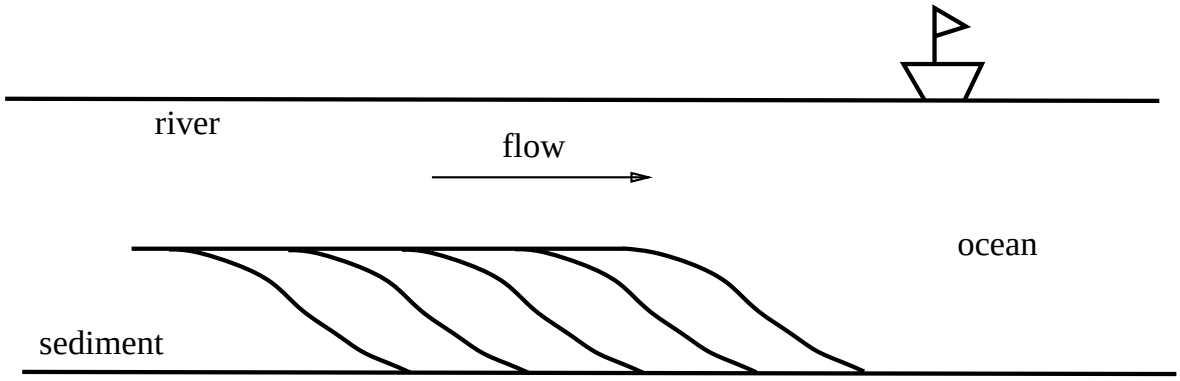

Figure 1.14: Sands (petroleum reservoir rocks) deposit on fairly steep slopes where rivers run into the ocean. xrf-river [NR]

Clays are more fine-grained materials (dirt) that are carried out to deeper water before they settle to make shale. Shale deposits tend to be layered somewhat more horizontally than sandstones. Specific locations of sand deposition change with the passing of storms and seasons, leaving a wood-grain-like appearance in the rock.

The river delta itself is a complicated, ever-changing arrangement of channels and bars, constantly moving along the coastline. At any one time the delta seems to be moving seaward as deposits are left, but later settling, compression, or elevation of sea level can cause it to move landward.

Sand is important because its porosity enables oil to accumulate and its permeability enables the oil to move to a well. Shale is important because it contains the products of former life on earth, and their hydrocarbons. These escape to nearby sands, but often not to the earth's surface, because of covering impermeable shales. The acoustic properties of sands and shales often overlap, though there is a slight tendency for shales to have a lower velocity than sands. Geophysicists on the surface see with seismic wavelengths ($\approx$ 30 meters) the final interbedded three-dimensional mixture of sands and shales.

Mixtures of sands and shales are called *clastic* rocks. The word *clast* means *break.* Clastic rocks are made from broken bits of crystalline rock. Most sedimentary rocks are clastic rocks. Most oil is found in clastic rocks. But much oil is also found in association with carbonates such as limestone. Carbonates are formed in shallow marine environments by marine organisms. Many carbonates (and clastics) contain oil that cannot be extracted because of lack of permeability. Permeability in carbonate rocks arises through several obscure processes. The seismologist knows carbonates as rocks with greater velocity than clastic rocks. Typically, a carbonate has a 20-50% greater velocity than a nearby clastic rock. Clastic rock sometimes contains limestone, in which case it is called *marl.*

Chrono-stratigraphy

Strange as it may seem, there is not universal agreement about the exact nature of seismic reflections. Physicists tend to think of the reflections as caused by the interface between rock types, as a sand-to-shale contact. The problem with this view is that sands and shales interlace in complex ways, both larger and smaller than the seismic wavelength. Many geologists, particularly a group known as *seismic stratigraphers,* have a different concept. (See *Seismic Stratigraphy—Applications to Hydrocarbon Exploration,* memoir 26 of the American Association of Petroleum Geologists). They have studied thousands of miles of reflection data along with well logs. They believe a reflection marks a constant geological time horizon. They assert that a long, continuous reflector could represent terrigenous deposition on one end and marine deposition on the other end with a variety of rock types in between. Data interpretation based on this assumption is called *chrono-stratigraphy.* The view of the seismic stratigrapher seems reasonable enough for areas that are wholly clastic, but when carbonates and other rocks are present, the physicist's view seems more appropriate. For further details, the book of Sheriff [1980] is recommended.

Chapter 2

Discrete Fourier transform

Happily, Fourier sums are exactly invertible: given the output, the input can be quickly found. Because signals can be transformed to the frequency domain, manipulated there, and then returned to the time domain, convolution and correlation can be done faster. Time derivatives can also be computed with more accuracy in the frequency domain than in the time domain. Signals can be shifted a fraction of the time sample, and they can be shifted back again exactly. In this chapter we will see how many operations we associate with the time domain can often be done better in the frequency domain. We will also examine some two-dimensional Fourier transforms.

2.1 FT AS AN INVERTIBLE MATRIX

A **Fourier sum** may be written

$$B(\omega) \quad = \quad \sum_t b_t \, e^{i\omega t} \quad = \quad \sum_t b_t \, Z^t \tag{2.1}$$

where the complex value Z is related to the real frequency ω by $Z = e^{i\omega}$. This Fourier sum is a way of building a continuous function of ω from discrete signal values b_t in the time domain. In this chapter we will study the computational tricks associated with specifying both time and frequency domains by a set of points. Begin with an example of a signal that is nonzero at four successive instants, (b_0, b_1, b_2, b_3). The transform is

$$B(\omega) \quad = \quad b_0 + b_1 Z + b_2 Z^2 + b_3 Z^3 \tag{2.2}$$

The evaluation of this polynomial can be organized as a matrix times a vector, such as

$$\begin{bmatrix} B_0 \\ B_1 \\ B_2 \\ B_3 \end{bmatrix} \quad = \quad \begin{bmatrix} 1 & 1 & 1 & 1 \\ 1 & W & W^2 & W^3 \\ 1 & W^2 & W^4 & W^6 \\ 1 & W^3 & W^6 & W^9 \end{bmatrix} \begin{bmatrix} b_0 \\ b_1 \\ b_2 \\ b_3 \end{bmatrix} \tag{2.3}$$

Observe that the top row of the matrix evaluates the polynomial at $Z = 1$, a point where also $\omega = 0$. The second row evaluates $B_1 = B(Z = W = e^{i\omega_0})$, where ω_0 is

some base frequency. The third row evaluates the Fourier transform for $2\omega_0$, and the bottom row for $3\omega_0$. The matrix could have more than four rows for more frequencies and more columns for more time points. I have made the matrix square in order to show you next how we can find the inverse matrix. The size of the matrix in (2.3) is $N = 4$. If we choose the base frequency ω_0 and hence W correctly, the inverse matrix will be

$$\begin{bmatrix} b_0 \\ b_1 \\ b_2 \\ b_3 \end{bmatrix} = 1/N \begin{bmatrix} 1 & 1 & 1 & 1 \\ 1 & 1/W & 1/W^2 & 1/W^3 \\ 1 & 1/W^2 & 1/W^4 & 1/W^6 \\ 1 & 1/W^3 & 1/W^6 & 1/W^9 \end{bmatrix} \begin{bmatrix} B_0 \\ B_1 \\ B_2 \\ B_3 \end{bmatrix} \tag{2.4}$$

Multiplying the matrix of (2.4) with that of (2.3), we first see that the diagonals are $+1$ as desired. To have the off diagonals vanish, we need various sums, such as $1+W+W^2+W^3$ and $1+W^2+W^4+W^6$, to vanish. Every element (W^6, for example, or $1/W^9$) is a unit vector in the complex plane. In order for the sums of the unit vectors to vanish, we must ensure that the vectors pull symmetrically away from the origin. A uniform distribution of directions meets this requirement. In other words, W should be the N-th root of unity, i.e.,

$$W = \sqrt[N]{1} = e^{2\pi i/N} \tag{2.5}$$

The lowest frequency is zero, corresponding to the top row of (2.3). The next-to-the-lowest frequency we find by setting W in (2.5) to $Z = e^{i\omega_0}$. So $\omega_0 = 2\pi/N$; and for (2.4) to be inverse to (2.3), the frequencies required are

$$\omega_k = \frac{(0, 1, 2, \ldots, N-1)\,2\pi}{N} \tag{2.6}$$

2.1.1 The Nyquist frequency

The highest frequency in equation (2.6), $\omega = 2\pi(N-1)/N$, is almost 2π. This frequency is twice as high as the Nyquist frequency $\omega = \pi$. The **Nyquist frequency** is normally thought of as the "highest possible" frequency, because $e^{i\pi t}$, for integer t, plots as $(\cdots, 1, -1, 1, -1, 1, -1, \cdots)$. The double Nyquist frequency function, $e^{i2\pi t}$, for integer t, plots as $(\cdots, 1, 1, 1, 1, 1, \cdots)$. So this frequency above the highest frequency is really zero frequency! We need to recall that $B(\omega) = B(\omega - 2\pi)$. Thus, all the frequencies near the upper end of the range (2.6) are really small negative frequencies. Negative frequencies on the interval $(-\pi, 0)$ were moved to interval $(\pi, 2\pi)$ by the matrix form of Fourier summation.

2.1.2 Laying out a mesh

In theoretical work and in programs, the definition $Z = e^{i\omega\Delta t}$ is often simplified to $\Delta t = 1$, leaving us with $Z = e^{i\omega}$. How do we know whether ω is given in radians per second or radians per sample? We may not invoke a cosine or an exponential unless

the argument has no physical dimensions. So where we see ω without Δt, we know it is in units of radians per sample.

In practical work, frequency is typically given in cycles or **Hertz**, f, rather than radians, ω (where $\omega = 2\pi f$). Here we will now switch to f. We will design a computer **mesh** on a physical object (such as a waveform or a function of space). We often take the mesh to begin at $t = 0$, and continue till the end $t_{\max}$ of the object, so the time range $t_{\text{range}} = t_{\max}$. Then we decide how many points we want to use. This will be the N used in the discrete Fourier-transform program. Dividing the range by the number gives a mesh interval Δt.

Now let us see what this choice implies in the frequency domain. We customarily take the maximum frequency to be the Nyquist, either $f_{\max} = .5/\Delta t$ Hz or $\omega_{\max} = \pi/\Delta t$ radians/sec. The frequency range f_{range} goes from $-.5/\Delta t$ to $.5/\Delta t$. In summary:

- $\Delta t \quad = \quad t_{\text{range}}/N$ is time **resolution**.
- $f_{\text{range}} \quad = \quad 1/\Delta t \quad = \quad N/t_{\text{range}}$ is frequency range.
- $\Delta f \quad = \quad f_{\text{range}}/N \quad = \quad 1/t_{\text{range}}$ is frequency **resolution**.

In principle, we can always increase N to refine the calculation. Notice that increasing N sharpens the time resolution (makes Δt smaller) but does not sharpen the frequency resolution Δf, which remains fixed. Increasing N increases the frequency *range,* but not the frequency *resolution.*

What if we want to increase the frequency resolution? Then we need to choose t_{range} larger than required to cover our object of interest. Thus we either record data over a larger range, or we assert that such measurements would be zero. Three equations summarize the facts:

$$\Delta t \; f_{\text{range}} = 1 \tag{2.7}$$

$$\Delta f \; t_{\text{range}} = 1 \tag{2.8}$$

$$\Delta f \; \Delta t = \frac{1}{N} \tag{2.9}$$

> Increasing *range* in the time domain increases *resolution* in the frequency domain and vice versa. Increasing **resolution** in one domain does not increase **resolution** in the other.

2.2 INVERTIBLE SLOW FT PROGRAM

Because Fourier sums are exactly invertible, some other things we often require can be done exactly by doing them in the frequency domain.

Typically, signals are real valued. But the programs in this chapter are for complex-valued signals. In order to use these programs, copy the real-valued signal into a complex array, where the signal goes into the real part of the complex numbers; the imaginary parts are then automatically set to zero.

There is no universally correct choice of **scale factor** in Fourier transform: choice of scale is a matter of convenience. Equations (2.3) and (2.4) mimic the Z-transform, so their scaling factors are convenient for the convolution theorem—that a product in the frequency domain is a convolution in the time domain. Obviously, the scaling factors of equations (2.3) and (2.4) will need to be interchanged for the complementary theorem that a convolution in the frequency domain is a product in the time domain. I like to use a scale factor that keeps the sums of squares the same in the time domain as in the frequency domain. Since I almost never need the scale factor, it simplifies life to omit it from the subroutine argument list. When a scaling program is desired, we can use a simple one like `scale()` (page 368). Complex-valued data can be scaled with `scale()` merely by doubling the value of `n`.

Fourier transform is just one of many transforms discussed in this book. In the case of most other transforms, the number of output values is different than the number of inputs. In addition, inverse transforms (and conjugate transforms), which will also be represented in code included in this book, transform in reverse, outputs to inputs. Finally, we will eventually combine transformations by addition or concatenation (one occurring after the other). All these considerations are expressed in the simple program `adjnull()`, which erases output before we begin. `Adjnull()` may seem like too trivial a function to put in a library routine, but at last count, 15 other routines in this book use it.

```
subroutine adjnull( adj, add, x, nx,  y, ny )
integer ix, iy,     adj, add,    nx,     ny
real                             x( nx), y( ny )
if( add == 0 )
        if( adj == 0 )
                do iy= 1, ny
                        y(iy) = 0.
        else
                do ix= 1, nx
                        x(ix) = 0.
return; end
```

2.2.1 The simple FT code

The `mple ft()` routine exhibits features found in many physics and engineering programs. For example, the time-domain signal (which I call "`tt()`"), has `nt` values subscripted, from `tt(1)` to `tt(nt)`. The first value of this signal `tt(1)` is located in real physical time at `t0`. The time interval between values is `dt`. The value of `tt(it)` is at time `t0+(it-1)*dt`. I do not use "`if`" as a pointer on the frequency axis because `if` is a keyword in most programming languages. Instead, I count along the frequency axis with a variable named `ie`.

```
subroutine simpleft( adj, add, t0,dt,tt,nt,  f0,df,  ff,nf)
```

```
integer it,ie,       adj, add,          nt,             nf
complex cexp, cmplx,                  tt(nt),         ff(nf)
real pi2, freq, time, scale,   t0,dt,        f0,df
call adjnull(        adj, add,       tt,nt*2,        ff,nf*2 )
                        pi2= 2. * 3.14159265;          scale = 1./sqrt( 1.*nt)
                        df = (1./dt) / nf
                        f0 =   - .5/dt
do ie = 1, nf {   freq= f0 + df*(ie-1)
do it = 1, nt {   time= t0 + dt*(it-1)
        if( adj == 0 )
                ff(ie)= ff(ie) + tt(it) * cexp(cmplx(0., pi2*freq*time)) * scale
        else
                tt(it)= tt(it) + ff(ie) * cexp(cmplx(0.,-pi2*freq*time)) * scale
        }}
return; end
```

The total frequency band is 2π radians per sample unit or $1/\Delta t$ Hz. Dividing the total interval by the number of points `nf` gives Δf. We could choose the frequencies to run from 0 to 2π radians/sample. That would work well for many applications, but it would be a nuisance for applications such as differentiation in the frequency domain, which require multiplication by $-i\omega$ including the **negative frequencies** as well as the positive. So it seems more natural to begin at the most negative frequency and step forward to the most positive frequency. Next, we must make a confusing choice.

2.3 SETTING UP THE FAST FOURIER TRANSFORM

Typically we **Fourier transform** seismograms about a thousand points long. Under these conditions another Fourier summation method works about a hundred times faster than those already given. Unfortunately, the faster Fourier transform program is not so transparently clear as the programs given earlier. Also, it is slightly less flexible. The speedup is so overwhelming, however, that the fast program is always used in routine work.

Flexibility may be lost because the basic fast program works with complex-valued signals, so we ordinarily convert our real signals to complex ones (by adding a zero imaginary part). More flexibility is lost because typical fast FT programs require the data length to be an integral power of 2. Thus geophysical datasets often have zeros appended (a process called "**zero pad**ding") until the data length is a power of 2. From time to time I notice clumsy computer code written to deduce a number that is a power of 2 and is larger than the length of a dataset. An answer is found by rounding up the logarithm to base 2. The more obvious and the quicker way to get the desired value, however, is with the simple Fortran function `pad2()`.

```
integer function pad2( n )
integer n
pad2 = 1
while( pad2 < n )
        pad2 = pad2 * 2
return; end
```

How fast is the fast Fourier transform method? The answer depends on the size

of the data. The matrix times vector operation in (2.3) requires N^2 multiplications and additions. That determines the speed of the slow transform. For the fast method the number of adds and multiplies is proportional to $N \log_2 N$. Since $2^{10} = 1024$, the speed ratio is typically 1024/10 or about 100. In reality, the fast method is not quite that fast, depending on certain details of overhead and implementation. In 1987 I tested the three programs on a 1024-point real signal and found times

`slowft`	153s
`polyft`	36s
`ftu`	.7s

Below is `ftu()`, a version of the **fast Fourier transform** program. There are many versions of the program—I have chosen this one for its simplicity. Considering the complexity of the task, it is remarkable that no auxiliary memory vectors are required; indeed, the output vector lies on top of the input vector. To run this program, your first step might be to copy your real-valued signal into a complex-valued array. Then append enough zeros to fill in the remaining space.

```
subroutine ftu( signi, nx, cx )
#   complex fourier transform with unitary scaling
#
#               1         nx          signi*2*pi*i*(j-1)*(k-1)/nx
#   cx(k)  =  -------- * sum cx(j) * e
#             sqrt(nx)   j=1             for k=1,2,...,nx=2**integer
#
integer nx, i, j, k, m, istep, pad2
real    signi, scale, arg
complex cx(nx), cmplx, cw, cdel, ct
if( nx != pad2(nx) )    call erexit('ftu: nx not a power of 2')
scale = 1. / sqrt( 1.*nx)
do i= 1, nx
        cx(i) = cx(i) * scale
j = 1;  k = 1
do i= 1, nx {
        if (i<=j) { ct = cx(j); cx(j) = cx(i); cx(i) = ct }
        m = nx/2
        while (j>m & m>1) { j = j-m; m = m/2 }          # "&" means .AND.
        j = j+m
        }
repeat {
        istep = 2*k;   cw = 1.;   arg = signi*3.14159265/k
        cdel = cmplx( cos(arg), sin(arg))
        do m= 1, k {
                do i= m, nx, istep
                        { ct=cw*cx(i+k);  cx(i+k)=cx(i)-ct;  cx(i)=cx(i)+ct }
                cw = cw * cdel
                }
        k = istep
        }  until(k>=nx)
return; end
```

The following two lines serve to Fourier transform a vector of 1024 complex-valued points, and then to **inverse Fourier transform** them back to the original data:

```
call ftu(  1., 1024, cx)
call ftu( -1., 1024, cx)
```

An engineering reference given at the end of this chapter contains many other versions of the FFT program. One version transforms real-valued signals to complex-valued frequency functions in the interval $0 \leq \omega < \pi$. Others that do not transform data on top of itself may be faster with specialized computer architectures.

EXERCISES:

1 Consider an even time function that is constant for all frequencies less than ω_0 and zero for all frequencies above ω_0. What is the rate of decay of amplitude with time for this function?

2 Waves spreading from a point source decay in energy as the area on a sphere. The amplitude decays as the square root of energy. This implies a certain decay in time. The time-decay rate is the same if the waves reflect from planar interfaces. To what power of time t do the signal amplitudes decay? For waves backscattered to the source from point reflectors, energy decays as distance to the minus fourth power. What is the associated decay with time?

2.3.1 Shifted spectrum

I have omitted a bit of theory here that is found in PVI.

For an FT matrix of arbitrary size N, the desired shift is $N/2$, so values at alternate points in the time axis are multiplied by -1. A subroutine for that purpose is `fth()`.

```
# FT a vector in a matrix, with first omega = - pi
#
subroutine  fth( adj,sign, m1, n12, cx)
integer i,       adj,      m1, n12
real sign
complex cx(m1,n12)
temporary complex temp(n12)
do i= 1, n12
        temp(i) = cx(1,i)
if( adj == 0)   { do i= 2, n12, 2
                        temp(i) =  -temp(i)
                  call ftu(  sign, n12, temp)
                }
else            { call ftu( -sign, n12, temp)
                  do i= 2, n12, 2
                        temp(i) =  -temp(i)
                }
do i= 1, n12
        cx(1,i) = temp(i)
return; end
```

To Fourier transform a 1024-point complex vector `cx(1024)` and then inverse transform it, you would

```
call fth( 0, 1., 1, 1024, cx)
call fth( 1, 1., 1, 1024, cx)
```

You might wonder about the apparent redundancy of using both the argument `conj` and the argument `sign`. Having two arguments instead of one allows us to define the *forward* transform for a *time* axis with the opposite sign as the forward transform for a *space* axis.

The subroutine `fth()` is somewhat cluttered by the inclusion of a frequently needed practical feature—namely, the facility to extract vectors from a matrix, transform the vectors, and then restore them into the matrix.

2.4 TWO-DIMENSIONAL FT

The program `fth()` is set up so that the vectors transformed can be either rows or columns of a two-dimensional array. To see how this works, recall that in **Fortran** a matrix allocated as `(n1,n2)` can be subscripted as a matrix `(i1,i2)` or as a long vector `(i1 + n1*(i2-1),1)`, and `call sub(x(i1,i2))` passes the subroutine a pointer to the `(i1,i2)` element. To transform an entire axis, the subroutines `ft1axis()` and `ft2axis()` are given. For a two-dimensional FT, we simply call both `ft1axis()` and `ft2axis()` in either order.

```
# 1D Fourier transform on a 2D data set along the 1-axis
#
subroutine  ft1axis( adj, sign1, n1,n2, cx)
integer i2,          adj,        n1,n2
complex cx(n1,n2)
real sign1
do i2= 1, n2
                call fth( adj, sign1, 1,n1, cx(1,i2))
return; end


# 1D Fourier transform on a 2D data set along the 2-axis
#
subroutine  ft2axis( adj, sign2, n1,n2, cx)
integer i1,          adj,        n1,n2
complex cx(n1,n2)
real    sign2
do i1= 1, n1
                call fth( adj, sign2, n1,n2, cx(i1,1))
return; end
```

I confess that there are faster ways to do things than those I have shown you above. When we are doing many FTs, for example, the overhead calculations done the first time should be saved for use on subsequent FTs, as in the subroutine `rocca()` included in IEI. Further, manufacturers of computers for heavy numerical use generally design special FT codes for their architecture. Although the basic fast FT used here ingeniously stores its output on top of its input, that feature is not compatible with vectorizing architectures.

2.4.1 Basics of two-dimensional Fourier transform

Before going any further, let us review some basic facts about **two-dimensional Fourier transform**. A two-dimensional function is represented in a computer as

numerical values in a matrix, whereas a one-dimensional Fourier transform in a computer is an operation on a vector. A 2-D Fourier transform can be computed by a sequence of 1-D Fourier transforms. We can first transform each column vector of the matrix and then each row vector of the matrix. Alternately, we can first do the rows and later do the columns. This is diagrammed as follows:

$$\begin{array}{ccc} p(t,\ x) & \longleftrightarrow & P(t,\ k_x) \\ \updownarrow & & \updownarrow \\ P(\omega,\ x) & \longleftrightarrow & P(\omega,\ k_x) \end{array}$$

The diagram has the notational problem that we cannot maintain the usual convention of using a lower-case letter for the domain of physical space and an upper-case letter for the Fourier domain, because that convention cannot include the mixed objects $P(t, k_x)$ and $P(\omega, x)$. Rather than invent some new notation, it seems best to let the reader rely on the context: the arguments of the function must help name the function.

An example of **two-dimensional Fourier transforms** on typical deep-ocean data is shown in Figure 2.1. In the deep ocean, sediments are fine-grained and deposit slowly in flat, regular, horizontal beds. The lack of permeable rocks such as sandstone severely reduces the potential for petroleum production from the deep ocean. The fine-grained shales overlay irregular, igneous, **basement rocks**. In the plot of $P(t, k_x)$, the lateral continuity of the sediments is shown by the strong spectrum at low k_x. The igneous rocks show a k_x spectrum extending to such large k_x that the deep data may be somewhat **spatially aliased** (sampled too coarsely). The plot of $P(\omega, x)$ shows that the data contains no low-frequency energy. The dip of the sea floor shows up in (ω, k_x)-space as the energy crossing the origin at an angle.

Altogether, the **two-dimensional Fourier transform** of a collection of seismograms involves only twice as much computation as the one-dimensional Fourier transform of each seismogram. This is lucky. Let us write some equations to establish that the asserted procedure does indeed do a 2-D Fourier transform. Say first that any function of x and t may be expressed as a superposition of sinusoidal functions:

$$p(t,x) \quad = \quad \int\int \ e^{-i\omega t + i k_x x} \ P(\omega, k_x) \ d\omega \ dk_x \tag{2.10}$$

The double integration can be nested to show that the temporal transforms are done first (inside):

$$\begin{aligned} p(t,x) \quad &= \quad \int \ e^{i\,k_x x} \ \left[\int \ e^{-i\omega t} \ P(\omega, k_x) \ d\omega \right] \ dk_x \\ &= \quad \int \ e^{i\,k_x x} \ P(t, k_x) \ dk_x \end{aligned}$$

The quantity in brackets is a Fourier transform over ω done for each and every k_x. Alternately, the nesting could be done with the k_x-integral on the inside. That

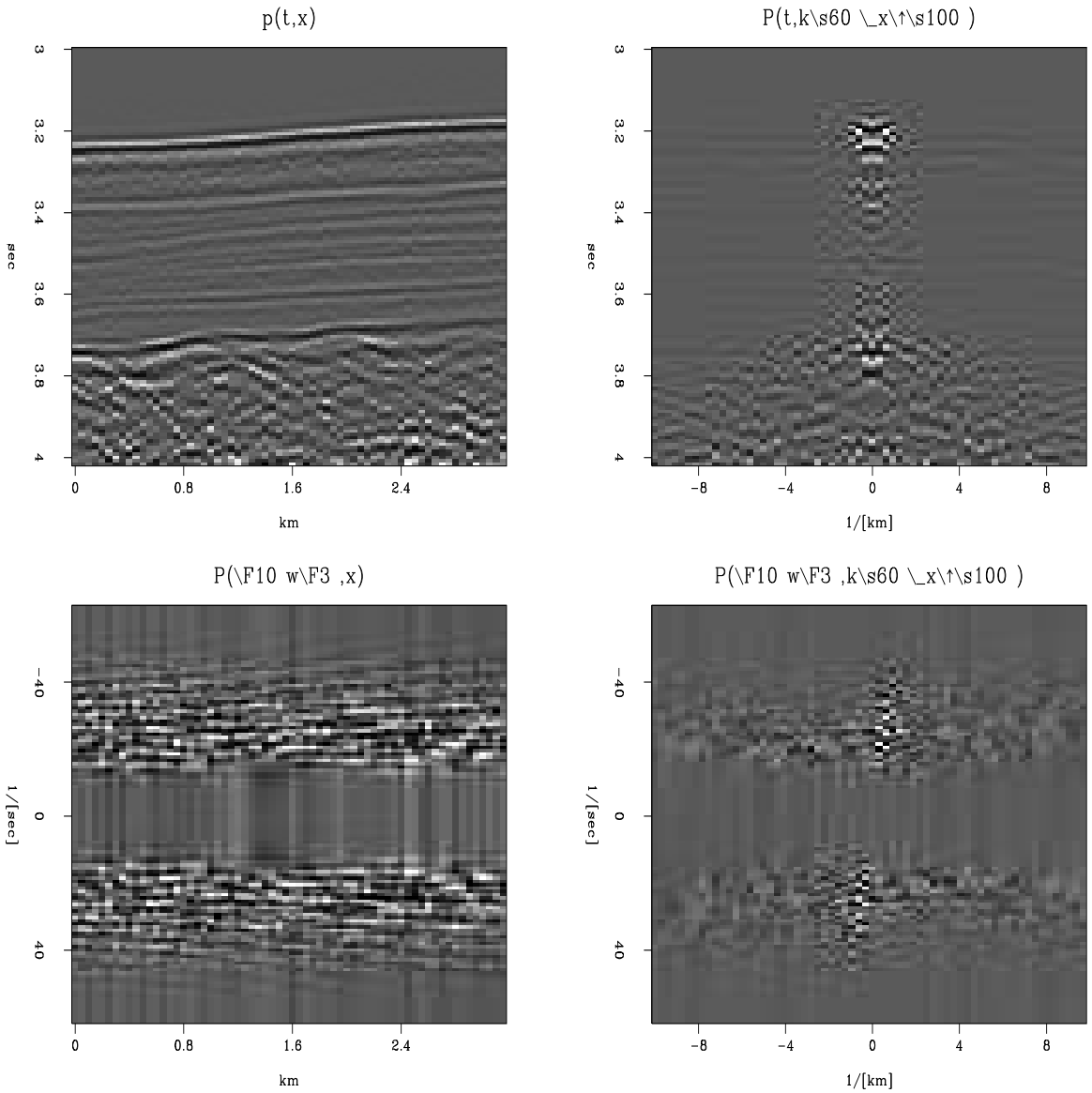

Figure 2.1: A deep-marine dataset $p(t,x)$ from Alaska (U.S. Geological Survey) and the *real* part of various Fourier transforms of it. Because of the long traveltime through the water, the time axis does not begin at $t = 0$. dft-plane4 [ER]

would imply rows first instead of columns (or vice versa). It is the separability of $\exp(-i\omega t + i\, k_x x)$ into a product of exponentials that makes the computation this easy and cheap.

2.4.2 Signs in Fourier transforms

In Fourier transforming t-, x-, and z-coordinates, we must choose a sign convention for each coordinate. Of the two alternative **sign conventions**, electrical engineers have chosen one and physicists another. While both have good reasons for their choices, our circumstances more closely resemble those of physicists, so we will use their convention. For the *inverse* Fourier transform, our choice is

$$p(t,x,z) \quad = \quad \int\int\int e^{-i\omega t + ik_x x + ik_z z}\, P(\omega, k_x, k_z)\, d\omega\, dk_x\, dk_z \tag{2.11}$$

For the *forward* Fourier transform, the space variables carry a *negative* sign, and time carries a *positive* sign.

Let us see the reasons why electrical engineers have made the opposite choice, and why we go with the physicists. Essentially, engineers transform only the time axis, whereas physicists transform both time and space axes. Both are simplifying their lives by their choice of sign convention, but physicists complicate their time axis in order to simplify their many space axes. The engineering choice minimizes the number of minus signs associated with the time axis, because for engineers, d/dt is associated with $i\omega$ instead of, as is the case for us and for physicists, with $-i\omega$. We confirm this with equation (2.11). Physicists and geophysicists deal with many more independent variables than time. Besides the obvious three space axes are their mutual combinations, such as midpoint and offset.

You might ask, why not make *all* the signs positive in equation (2.11)? The reason is that in that case waves would not move in a positive direction along the space axes. This would be especially unnatural when the space axis was a radius. Atoms, like geophysical sources, always radiate from a point to infinity, not the other way around. Thus, in equation (2.11) the sign of the spatial frequencies must be opposite that of the temporal frequency.

The only good reason I know to choose the engineering convention is that we might compute with an array processor built and microcoded by engineers. Conflict of sign convention is not a problem for the programs that transform complex-valued time functions to complex-valued frequency functions, because there the sign convention is under the user's control. But sign conflict does make a difference when we use any program that converts real-time functions to complex frequency functions. The way to live in both worlds is to imagine that the frequencies produced by such a program do not range from 0 to $+\pi$ as the program description says, but from 0 to $-\pi$. Alternately, we could always take the complex conjugate of the transform, which would swap the sign of the ω-axis.

2.4.3 Examples of 2-D FT

An example of a **two-dimensional Fourier transform** of a pulse is shown in Figure 2.2. Notice the location of the pulse. It is closer to the time axis than the

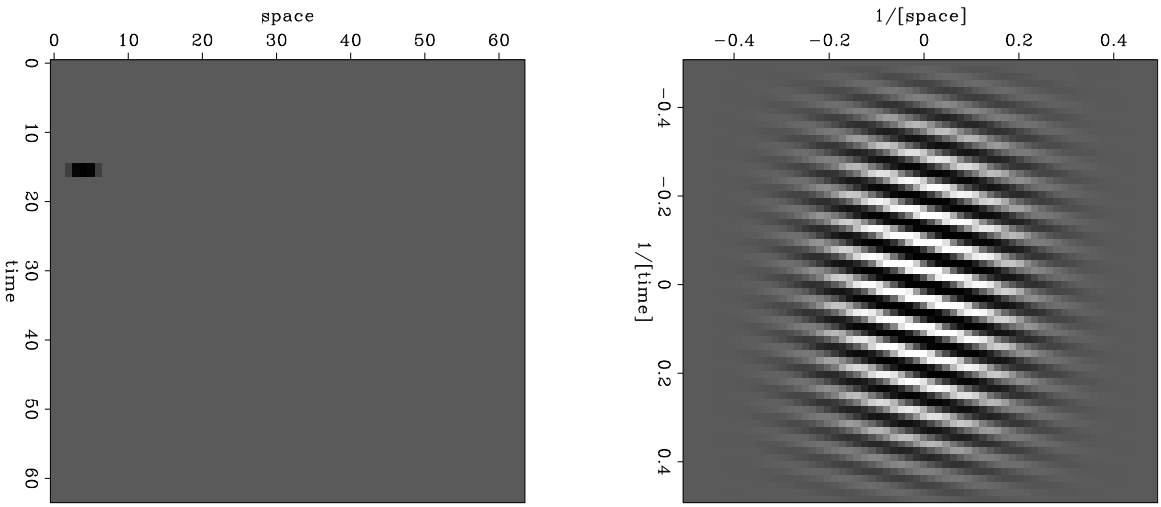

Figure 2.2: A broadened pulse (left) and the real part of its FT (right). dft-ft2dofpulse [ER]

frequency axis. This will affect the real part of the FT in a certain way (see exercises). Notice the broadening of the pulse. It was an impulse smoothed over time (vertically) by convolution with (1,1) and over space (horizontally) with (1,4,6,4,1). This will affect the real part of the FT in another way.

Another example of a two-dimensional Fourier transform is given in Figure 2.3. This example simulates an impulsive air wave originating at a point on the x-axis. We see a wave propagating in each direction from the location of the source of the wave. In Fourier space there are also two lines, one for each wave. Notice that there are other lines which do not go through the origin; these lines are called "**spatial alias**es." Each actually goes through the origin of another square plane that is not shown, but which we can imagine alongside the one shown. These other planes are periodic replicas of the one shown.

EXERCISES:

1 Write `ftlag()` starting from `ftlagslow()` and `fth()`.

2 Most time functions are real. Their imaginary part is zero. Show that this means that $F(\omega, k)$ can be determined from $F(-\omega, -k)$.

3 What would change in Figure 2.2 if the pulse were moved (a) earlier on the t-axis, and (b) further on the x-axis? What would change in Figure 2.2 if instead the time axis were smoothed with (1,4,6,4,1) and the space axis with (1,1)?

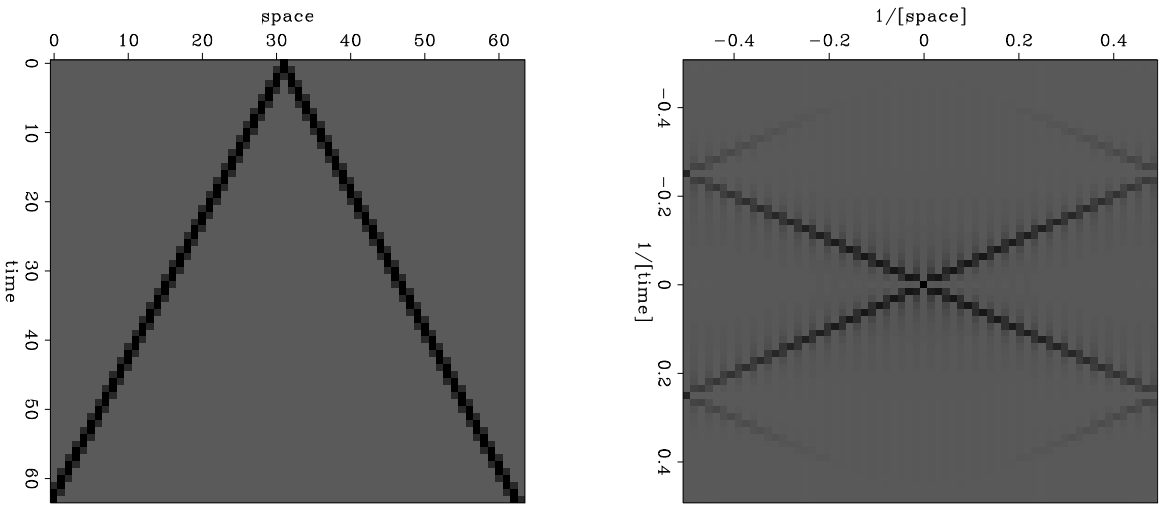

Figure 2.3: A simulated air wave (left) and the amplitude of its FT (right). dft-airwave [ER]

4 What would Figure 2.3 look like on an earth with half the earth velocity?

5 Numerically (or theoretically) compute the two-dimensional spectrum of a plane wave $[\delta(t-px)]$, where the plane wave has a randomly fluctuating amplitude: say, rand(x) is a random number between ± 1, and the randomly modulated plane wave is $[(1 \ + \ .2\,\text{rand}(x))\,\delta(t-px)]$.

6 Explain the horizontal "layering" in Figure 2.1 in the plot of $P(\omega, x)$. What determines the "layer" separation? What determines the "layer" slope?

REFERENCES

Special issue on fast Fourier transform, June 1969: IEEE Trans. on Audio and Electroacoustics (now known as IEEE Trans. on Acoustics, Speech, and Signal Processing), **AU-17**, entire issue (66-172).

Chapter 3

Wide-angle migration methods

The four methods of migration of reflection seismic data that are described here are all found in modern production environments. As a group they handle wide-angle rays easily. As a group they are used less successfully to deal with lateral velocity variation. They are all based on Fourier transforms.

3.1 PLANE-WAVE SUPERPOSITION

One of the main ideas in Fourier analysis is that an impulse function (a delta function) can be constructed by the superposition of sinusoids (or complex exponentials). In the study of time series this construction is used for the *impulse response* of a filter. In the study of functions of space, it is used to make a physical point source.

Taking time and space together, Fourier components can be interpreted as monochromatic plane waves. Physical optics (and with it reflection seismology) becomes an extension to filter theory. In this section we learn the mathematical form, in Fourier space, of the Huygens secondary source. It is a two-dimensional (2-D) filter for spatial extrapolation of wavefields.

3.1.1 Migration improves horizontal resolution

In principle, migration converts hyperbolas to points. In practice, hyperbolas don't collapse to a point, they collapse to a *focus.* A focus has measurable dimensions. Migration is said to be "good" because it increases spatial resolution. It squeezes a large hyperbola down to a tiny focus. To quantitatively describe the improvement of migration, the size of the hyperbola and the size of the focus must be defined. Figure 3.1 shows various ways of measuring the size of a hyperbola.

The hyperbola carries an impulsive arrival. So the ω-bandwidth of the hyperbola is roughly given by the zero crossings on the time axis of the main energy burst. I'll mention 50 Hz as a typical value, though you could encounter values four times higher or four times lower. Knowledge of a seismic velocity determines depth resolution. I'll

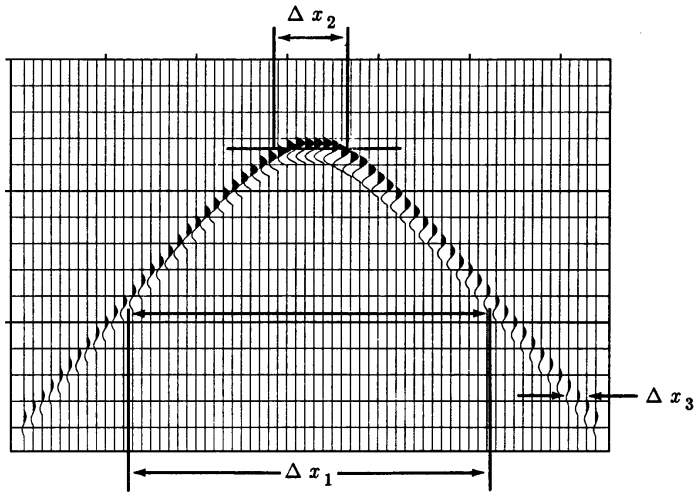

Figure 3.1: Measurements of width parameters of a hyperbola. omk-fwidth [NR]

suggest 3 km/sec, though once again you could encounter velocities four times greater or four times less. These values imply a seismic wavelength of $v/f = 60$ meters. But the effective seismic wavelength is half the actual wavelength. The half comes from halving the velocity v in exploding reflector calculations, or equivalently, from realizing that the seismic wavelength is divided equally into upgoing and downgoing parts. Resolving power is customarily defined as about half the effective wavelength or about 15 meters. (Whether seismic resolution should be *half* the effective wavelength or a smaller fraction is an issue that involves signal-to-noise considerations outside our present study).

The lateral resolution requires estimates of hyperbola width and focus width. Figure 3.1 shows three hyperbola widths. The widest, Δx_1, includes about three-quarters of the energy in the hyperbola. Next is the width Δx_2, called the *Fresnel Zone.* It is measured across the hyperbola at the time when the first arrival has just changed polarity. Third is the smallest measurable width, found far out on a flank. This width, Δx_3, is the shortest horizontal wavelength to be found. Resolution is the study of the size of error, and it is not especially useful to be precise about the error in the error. The main idea is that $\Delta x_1 > \Delta x_2 > \Delta x_3$. The bandwidth of the spatial k_x spectrum is roughly $1/\Delta x_3$. How small a focus can migration make? It will be limited by the available bandwidth in the k_x spectrum. The size of the focus will be about the same as Δx_3.

Figure 3.2 shows the geometry of the Fresnel zone concept. A Fresnel zone is an intercept of a spherical wave with a plane. The intercept is defined when the spherical wave penetrates the plane to a depth of a half wavelength. What is the meaning of the Fresnel width Δx_2? Imagine yourself in Berlin. There was a wall there. You could not go near it. Imagine a hole in the wall. You are shouting to a friend on the opposite side. How does the loudness of the sound depend on the size of the hole ΔX? It is not obvious, but it is well known, both theoretically and

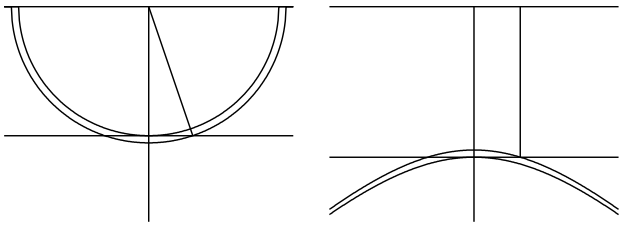

Figure 3.2: Fresnel zone in (x, z)-space (left) and in (x, t)-space (right). omk-fresnel [ER]

experimentally, that holes larger than the Fresnel zone cause little attenuation, but smaller holes restrict the sound in proportion to their size.

Wave propagation is a convolutional filter that smears information from a region Δx_2 along a reflector (or Δx_1 in the subsurface). Migration, the reverse of wave propagation, is the deconvolution operation. The final amount of lateral resolution is limited by the spatial bandwidth of the data.

Migration may be called for even where reflectors show no dip. When a well site is to be chosen within an accuracy of less than Δx_2 then the interpreter is looking at subtle changes in amplitude or waveform along the reflector. Migration causes these amplitude and waveform variations to change and to move horizontally along the reflector. The distance moved is about equal the Fresnel zone.

A basic fact of seismology is the resolution limitation caused by the increase with depth of the seismic velocity. What happens is that as the waves get deeper into the earth, their spatial wavelengths get longer because of the increasing velocity. The case of vertical resolution is simply this: longer wavelengths, less resolution. The case of horizontal resolution is similar, but the horizontal wavelength is directly measurable at the earth's surface. Figure 3.3 demonstrates this. Hyperboloids from

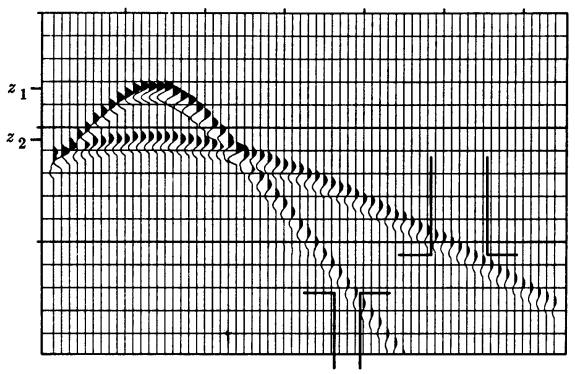

Figure 3.3: Hyperboloids for an earth of velocity increasing with depth. Observable lateral wavelengths get longer with increasing depth. Thus lateral resolving power decreases with depth. omk-hyp2 [NR]

shallow and deep scatterers are shown. Shallow hyperbolas have early tops and steep asymptotes. Deep scatterers have late tops and less steep asymptotes. The less steep asymptotes have longer horizontal wavelength. Horizontal wavelengths measured at the surface are unchanged at depth, even though velocity increases with depth. Thus,

lateral spatial resolution gets worse with depth. Compounding the above reason for decreasing resolution is the loss of high-frequency energy at late travel time.

3.1.2 Rays and fronts

Figure 3.4 depicts a ray moving down into the earth at an angle θ from the vertical.

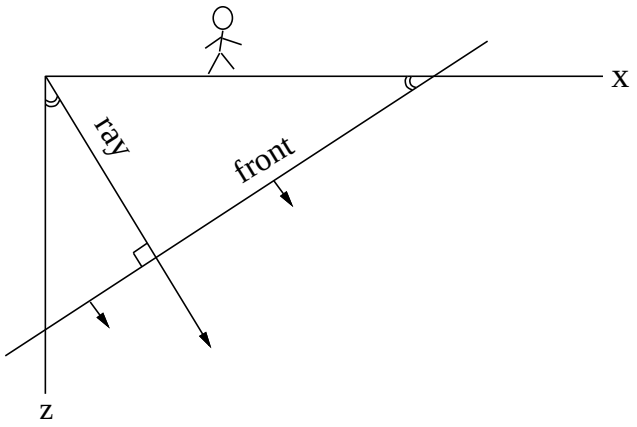

Figure 3.4: Downgoing ray and wavefront. omk-front [NR]

Perpendicular to the ray is a wavefront. By elementary geometry the angle between the wavefront and the earth's surface is also θ. The ray increases its length at a speed v. The speed that is observable on the earth's surface is the intercept of the wavefront with the earth's surface. This speed, namely $v/\sin\theta$, is faster than v. Likewise, the speed of the intercept of the wavefront and the vertical axis is $v/\cos\theta$. A mathematical expression for a straight line would be

$$z \;=\; z_0 \;-\; x\ \tan\theta \tag{3.1}$$

like that shown to be the wavefront in Figure 3.4.

In this expression z_0 is the intercept between the wavefront and the vertical axis. To make the intercept move downward, replace it by the appropriate velocity times time:

$$z \;=\; v\,\frac{t}{\cos\theta} \;-\; x\ \tan\theta \tag{3.2}$$

Solving for time gives

$$t(x,z) \;=\; \frac{z}{v}\ \cos\theta \;+\; \frac{x}{v}\ \sin\theta \tag{3.3}$$

Equation (3.3) tells the time that the wavefront will pass any particular location (x, z). The expression for a shifted waveform of arbitrary shape is $f(t - t_0)$. Using (3.3) to define the time shift t_0 gives an expression for a wavefield that is some waveform moving on a ray.

$$\text{moving wavefield} \;=\; f\left(\ t \;-\; \frac{x}{v}\ \sin\theta \;-\; \frac{z}{v}\ \cos\theta\right) \tag{3.4}$$

3.1.3 Waves in Fourier space

Arbitrary functions can be made from the superposition of sinusoids. Sinusoids and complex exponentials often occur. One reason they occur is that they are the solutions to linear partial differential equations (PDEs) with constant coefficients. The PDEs arise because most laws of physics are expressible as PDEs.

Using Fourier integrals on time functions we encounter the *Fourier kernel* $\exp(-i\omega t)$. Specializing the arbitrary function in equation (3.4) to be the real part of the function $\exp[-i\omega(t - t_0)]$ gives

$$\text{moving cosine wave} \quad = \quad \cos\left[\ \omega\left(\frac{x}{v}\ \sin\,\theta\ +\ \frac{z}{v}\ \cos\,\theta\ -\ t\ \right)\ \right] \tag{3.5}$$

To use Fourier integrals on the space-axis x the spatial angular frequency must be defined. Since we will ultimately encounter many space axes (three for shot, three for geophone, also the midpoint and offset), the convention will be to use a subscript on the letter k to denote the axis being Fourier transformed. So k_x is the angular spatial frequency on the x-axis and $\exp(ik_x x)$ is its Fourier kernel. For each axis and Fourier kernel there is the question of the sign of i. The sign convention used here is the one used in most physics books, namely, the one that agrees with equation (3.5). With this convention, a wave moves in the *positive* direction along the space axes. Thus the Fourier kernel for (x, z, t)-space will be taken to be

$$\text{Fourier kernel} \ = \ e^{i\,k_x x}\ e^{i\,k_z z}\ e^{-\,i\omega t} \ = \ \exp[i(k_x x\ +\ k_z z\ -\ \omega t)] \tag{3.6}$$

Now for the whistles, bells, and trumpets. Equating (3.5) to the real part of (3.6), physical angles and velocity are related to Fourier components. These relations should be memorized!

Angles and Fourier Components	
$\sin\theta = \dfrac{v\ k_x}{\omega}$	$\cos\theta = \dfrac{v\ k_z}{\omega}$

(3.7)

Equally important is what comes next. Insert the angle definitions into the familiar relation $\sin^2\theta + \cos^2\theta = 1$. This gives a most important relationship, seen earlier as the *dispersion relation of the scalar wave equation.*

$$k_x^2\ +\ k_z^2 \quad = \quad \frac{\omega^2}{v^2} \tag{3.8}$$

The importance of (3.8) is that it enables us to make the distinction between an arbitrary function and a chaotic function that actually is a wavefield. Take any function $p(t, x, z)$. Fourier transform it to $P(\omega, k_x, k_z)$. Look in the (ω, k_x, k_z)-volume for any nonvanishing values of P. You will have a wavefield if and only if all nonvanishing

P have coordinates that satisfy (3.8). Even better, in practice the (x, t)-dependence at $z = 0$ is usually known, but the z-dependence is not. Then the z-dependence is found by assuming P is a wavefield, so the z-dependence is inferred from (3.8).

3.1.4 The input-output relation

At the heart of the migration process is the operation of downward continuing data. Given the input data on the plane of the earth's surface $z = 0$, we must manufacture the data that could be recorded at depth z. This is most easily done in the Fourier domain. Mathematically shifting on the z-axis is like shifting on the time t-axis. To shift on time by an amount t_0 we multiply by $\exp(i\omega t_0)$ and to shift on depth by an amount z_0 we multiply by $\exp(ik_z z_0)$. It is not quite this trivial however: the data field is not evidently a function of k_z because we do not have data given on a z-axis so we cannot simply Fourier transform it to k_z. Instead we have

$$P(\omega, k_x, z) \quad = \quad P(\omega, k_x, 0)\; e^{i\, k_z(\omega, k_x) z} \tag{3.9}$$

Since the operation is a multiplication in the Fourier domain, it may be described as the engineering diagram in Figure 3.5.

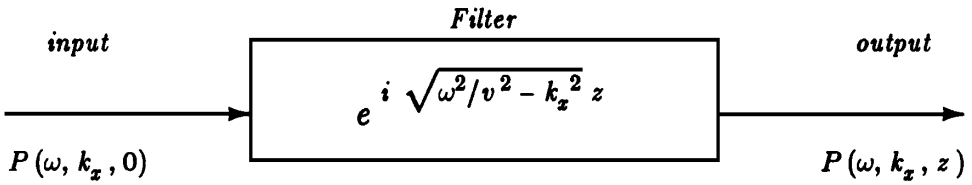

Figure 3.5: omk-inout [NR]

Downward continuation is a product relationship in both the ω-domain and the k_x-domain. What does the filter look like in the time and space domain? It turns out like a cone, that is, it is roughly an impulse function of $x^2 + z^2 - v^2t^2$. More precisely, it is the Huygens secondary wave source that was exemplified by ocean waves entering a gap through a storm barrier. Adding up the response of multiple gaps in the barrier would be convolution over x. Superposing many incident ocean waves would be convolution over t.

Now let us see why the downward continuation filter has the mathematical form stated. Every point in the (ω, k_x)-plane refers to a sinusoidal plane wave. The variation with depth will also be sinusoidal, namely $\exp(ik_z z)$. The value of k_z for the plane wave is found simply by solving equation (3.8):

$$k_z \quad = \quad \pm\sqrt{\frac{\omega^2}{v^2} - k_x^2} \tag{3.10}$$

$$\quad = \quad \pm\,\frac{\omega}{v}\,\sqrt{1 - \frac{v^2\,k_x^2}{\omega^2}} \tag{3.11}$$

$$= \quad \pm \frac{\omega}{v} \cos\theta \tag{3.12}$$

Choice of the *plus* sign means that $\exp(-i\omega t + i k_z z)$ is a *down*going wave (because the phase will stay constant if z increases as t increases). Choice of a *minus* sign makes the wave *up*coming. The exploding-reflector concept requires upcoming waves, so we nearly always use the minus sign, whether we are migrating or modeling.

Mathematically we can imagine an arbitrary function of t, x, and z. Its three-dimensional Fourier transform fills a volume in the space of ω, k_x, and k_z. This arbitrary function is not a wavefield unless it vanishes everywhere except the cone-shaped surface $k_x^2+k_z^2 = \omega^2/v^2$ given by the wave equation. Thus equation (3.9) makes sense even though we cannot Fourier transform data over the z-axis because we don't observe data along the z-axis. It makes sense because if we know the mathematical function is a wavefield and if we know its Fourier transform over ω and k_x, then we know its Fourier transform at any k_z and we can "delay" it in z (downward shift) by multiplying by $\exp(ik_z z)$.

The input-output filter, being of the form $e^{i\phi}$, appears to be a phase-shifting filter with *no amplitude scaling.* This bodes well for our plans to deconvolve. It means that signal-to-noise power considerations will be much less relevant for migration than for ordinary filtering.

EXERCISES:

1 Suppose that you are able to observe some shear waves at ordinary seismic frequencies. Is the spatial resolution better, equal, or worse than usual? Why?

2 Scan this book for hyperbolic arrivals on field data and measure the Fresnel zone width. Where zero offset recordings are not made, a valid approximation is to measure Δx_2 along a *tilted* line.

3 Evolution of a wavefield with time is described by

$$p(x,z,t) \;=\; \int\int \Big[\, P(k_x,k_z,t=0)\, e^{-i\omega(k_x,k_z)t} \Big]\; e^{ik_x x + ik_z z} dk_x\, dk_z \tag{3.13}$$

Let $P(k_x,k_z,0)$ be constant, signifying a point source at the origin in (x,z)-space. Let t be very large, meaning that phase $= \phi = [-\omega(k_x,k_z) + k_x\,(x/t) + k_z\,(z/t)]t$ in the integration is rapidly alternating with changes in k_x and k_z. Assume that the only significant contribution to the integral comes when the phase is stationary, that is, where $\partial\phi/\partial k_x$ and $\partial\phi/\partial k_z$ both vanish. Where is the energy in (x,z,t)-space?

4 Downward continuation of a wave is expressed by

$$p(x,z,t) \;=\; \int\int \Big[\, P(k_x,z=0,\omega)\; e^{ik_z(\omega,k_x)z} \Big]\; e^{-i\omega t + ik_x x}\; d\omega\, dk_x \tag{3.14}$$

Let $P(k_x,0,\omega)$ be constant, signifying a point source at the origin in (x,t)-space. Where is the energy in (x,z,t)-space?

3.1.5 Travel-time depth

Conceptually, the output of a migration program is a picture in the (x, z)-plane. In practice the vertical axis is almost never depth z; it is the *vertical travel time* τ. In a constant-velocity earth the time and the depth are related by a simple scale factor. The meaning of the scale factor is that the (x, τ)-plane has a vertical exaggeration compared to the (x, z)-plane. In reconnaissance work, the vertical is often exaggerated by about a factor of five. By the time prospects have been sufficiently narrowed for a drill site to be selected, the vertical exaggeration factor in use is likely to be about unity (no exaggeration).

The travel-time depth τ is usually defined to include the time for both the wave going down and the wave coming up. The factor of two thus introduced quickly disappears into the rock velocity. Recall that zero-offset data sections are generally interpreted as exploding-reflector wavefields. To make the correspondence, the rock velocity is cut in half for the wave analysis:

$$\tau \quad = \quad \frac{2\,z}{v_{\text{true}}} \quad = \quad \frac{z}{v_{\text{half}}} \tag{3.15}$$

The first task in interpretation of seismic data is to figure out the approximate numerical value of the vertical exaggeration. It probably won't be printed on the data header because the seismic velocity is not really known. Furthermore, the velocity usually *increases* with depth, which means that the vertical exaggeration *decreases* with depth. For velocity-stratified media, the time-to-depth conversion formula is

$$\tau(z) \quad = \quad \int_0^z \frac{dz}{v(z)} \qquad \text{or} \qquad \frac{d\tau}{dz} \quad = \quad \frac{1}{v} \tag{3.16}$$

3.2 SUMMATION AND SUPERPOSITION OF CONICS

The methods of hyperbola summation and semicircle superposition are the most comprehensible of all known methods.

Recall the equation for a conic section, that is, a circle in (x, z)-space or a hyperbola in (x, t)-space. Converting to travel-time depth τ

$$x^2 \;+\; z^2 \quad = \quad v^2\, t^2 \tag{3.17}$$

$$\frac{x^2}{v^2} \;+\; \tau^2 \quad = \quad t^2 \tag{3.18}$$

Figure 3.6, which is from Schneider's classic paper [1971], illustrates the *semicircle-superposition* method. Taking the data field to contain a few impulse functions, the output should be a superposition of the appropriate semicircles. Each semicircle denotes the spherical-reflector earth model that would be implied by a dataset with a single pulse. Taking the data field to be one thousand seismograms of one thousand

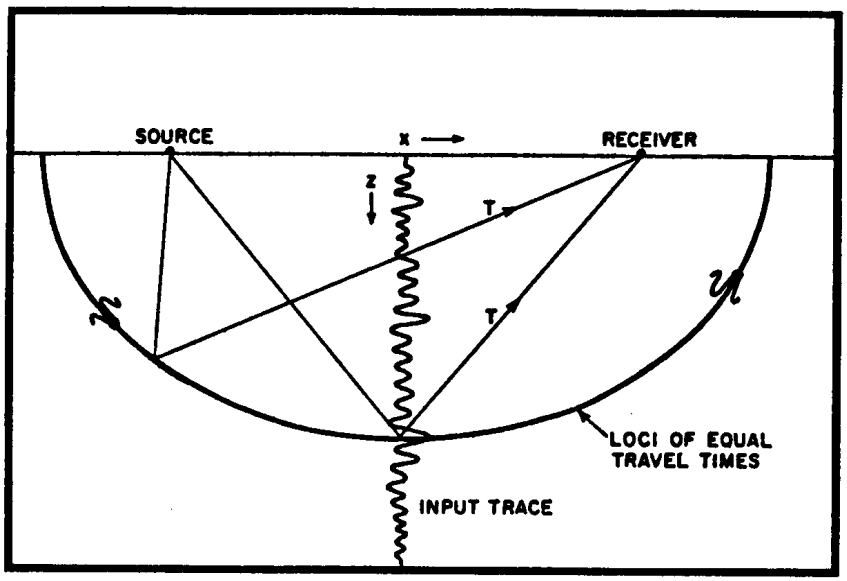

Figure 3.6: The process may be described in numerous ways. Two very simple and equally valid representations are indicated in Figures 3.6 and 3.7. Shown here is a representation of the process in terms of what happens to a single input trace plotted in depth (time may also be used) midway between its source and receiver. Each amplitude value of this trace is mapped into the subsurface along a curve representing the loci of points for which the travel time from source to reflection point to receiver is constant. If the velocity is constant, these curves are ellipses with source and receiver as foci. The picture produced by this operation is simply a wavefront chart modulated by the trace amplitude information. This clearly is not a useful image in itself, but when the map is composited with similar maps from neighboring traces (and common-depth-point traces of different offsets), useful subsurface images are produced by virtue of constructive and destructive interference between wavefronts in the classical Huygens sense. For example, wavefronts from neighboring traces will all intersect on a diffraction source, adding constructively to produce an image of the diffractor as a high-amplitude blob whose (z, x) resolution is controlled by the pulse bandwidth and the horizontal aperture of the array of neighboring traces composited. For a reflecting surface, on the other hand, wavefronts from adjacent traces are tangent to the surface and produce an image of the reflector by constructive interference of overlapping portions of adjacent wavefronts. In subsurface regions devoid of reflecting and scattering bodies, the wavefronts tend to cancel by random addition. (figure and caption from Schneider, W. A., 1971 [by permission]) omk-schneider [NR]

points each, then the output is a superposition of one million semicircles. Since a seismogram has both positive and negative polarities, about half the semicircles will be superposed with negative polarities. The resulting superposition could look like almost anything. Indeed, the semicircles might mutually destroy one another almost everywhere except at one isolated impulse in (x, τ)-space. Should this happen you might rightly suspect that the input data section in (x, t)-space is a Huygens secondary source, namely, energy concentrated along a hyperbola. This leads us to the *hyperbola-summation* method.

The *hyperbola-summation* method of migration is depicted in Figure 3.7. The idea is to create one point in (x, τ)-space at a time, unlike in the semicircle method, where each point in (x, τ)-space is built up bit by bit as the one million semicircles are stacked together. To create one fixed point in the output (x, τ)-space, imagine a hyperbola, equation (3.18), set down with its top on the corresponding position of (x, t)-space. All data values touching the hyperbola are added together to produce a value for the output at the appropriate place in (x, τ)-space. In the same way, all other locations in (x, τ)-space are filled. We can wonder whether the hyperbola-migration method is better or worse than or equivalent to the semicircle method.

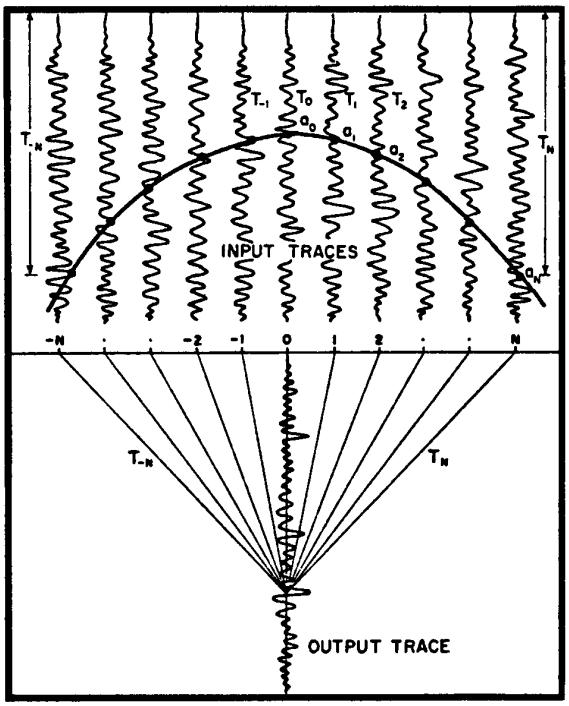

Figure 3.7: A second description of the process is provided here. The process is represented in terms of how an output trace is developed from an ensemble of input traces, shown as CDP-stacked traces in the upper half of the figure. The output in the lower half reflects how each amplitude value at (x, z) is obtained by summing input amplitudes along the traveltime curve shown. This curve defines a diffraction hyperbola. If a diffraction source existed in the subsurface at the output point shown, then a large amplitude would result. The process also works for reflectors since a reflector may be regarded as a continuum of diffracting elements whose individual images merge to produce a smooth continuous boundary. (figure and caption from Schneider, 1971) omk-schneider2 [NR]

The opposite of data processing or building models from data is constructing synthetic data from models. With a slight change, the above two processing programs can be converted to modeling programs. Instead of *hyperbola summation* or *semicircle*

superposition, you do *hyperbola superposition* or *semicircle summation.* We can also wonder whether the processing programs really are inverse to the modeling programs. Some factors that need to be considered are (1) the angle-dependence of amplitude (the obliquity function) of the Huygens waveform, (2) spherical spreading of energy, and (3) the phase-shift on the Huygens waveform. It turns out that results are reasonably good even when these complicating factors are ignored.

As other methods of migration were developed, the deficiencies of the earlier methods were more clearly understood and found to be largely correctable by careful implementation. One advantage of the later methods is that they implement true all-pass filters. Such migrations preserve the general appearance of the data. This suggests restoration of high frequencies, which tend to be destroyed by hyperbolic integrations. Work with the Kirchhoff diffraction integral by Trorey [1970] and Hilterman [1970] led to forward modeling programs. Eventually (Schneider [1977]) this work suggested quantitative means of bringing hyperbola methods into agreement with other methods, at least for constant velocity. Common terminology nowadays is to refer to any hyperbola or semicircular method as a Kirchhoff method, although, strictly speaking, the Kirchhoff integral applies only in the constant-velocity case.

3.2.1 Hyperbola summation refined into the Kirchhoff method

Schneider [1978] states the analytic representation for the Huygens secondary wavelet

$$\mathrm{FT}^{-1}(e^{i k_z z}) \quad = \quad \frac{1}{\pi} \frac{\partial}{\partial z_0} \frac{\mathrm{step}(t - r/v)}{\sqrt{t^2 - r^2/v^2}} \tag{3.19}$$

where r is the distance $\sqrt{x^2 + (z - z_0)^2}$ between the (exploding reflector) source and the receiver. The function (3.19) contains a pole and the derivative of a step function. Because of the infinities it really cannot be graphed. But from the mathematical form you immediately recognize that the disturbance concentrates on the expected cone. The derivative of the step function gives a positive impulsive arrival on the cone. The derivative of the inverse square root gives the impulse a tail of negative polarity decaying with a $-3/2$ power. The cosine obliquity arises because the derivative is a z derivative and not an r derivative.

Equation (3.19) states the *two*-dimensional Huygens wavelet, not the *three*-dimensional wavelet (which differs in some minor aspects). Although waves from point sources are mainly spherical, the focusing of bent layers is mainly a two-dimensional focusing, i.e., bent layers are more like cylinders than spheres.

You might wonder why anyone would prefer approximations, given the exact inverse transform (3.19). The difficulty of graphing (3.19) shows up in practice as a difficulty in convolving it with data. That is why early Kirchhoff migrations were generally recognizable by precursor noise above a flat sea floor. Chapters 4, 8, and 9, are largely devoted to extensions of (3.19) that are valid with variable velocity and that are better representations on a data mesh.

In the Fourier domain, the Huygens secondary source function is simple and smooth. It is a straightforward matter to evaluate the function on a rectangular mesh and inverse transform with `ft1axis()` (page 32) and `ft2axis()` (page 32). Figure 3.8 shows the result on a 256 $\times$ 64 point mesh. (In practice the mesh

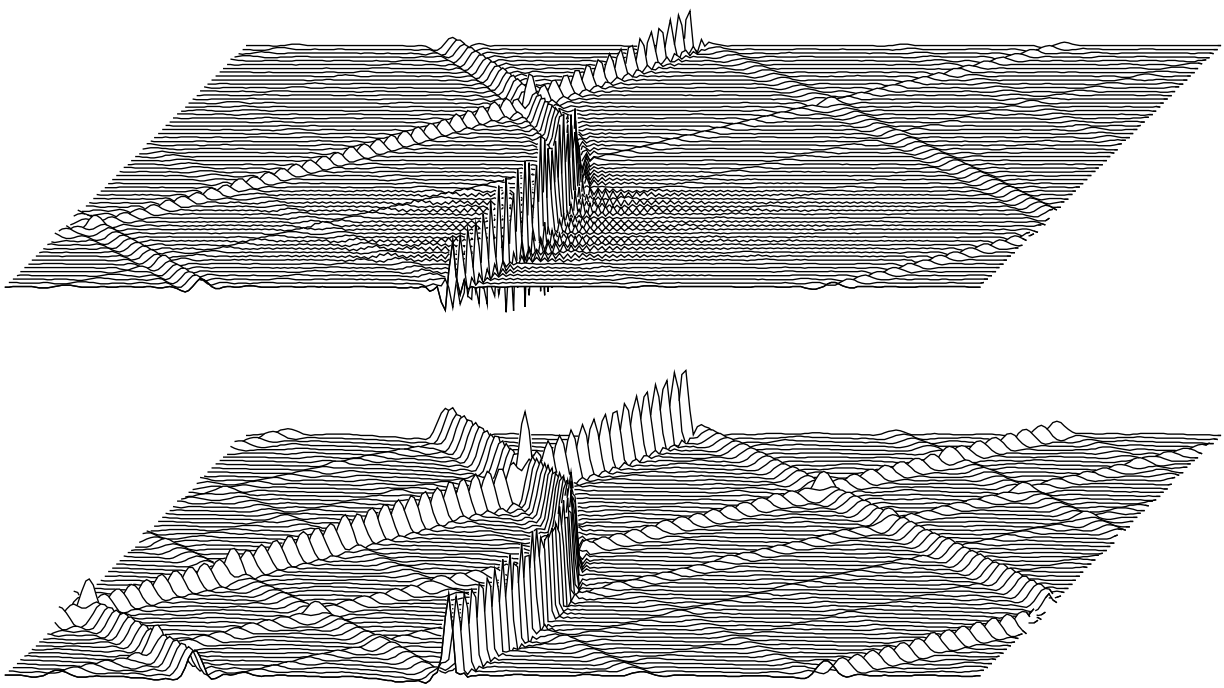

Figure 3.8: The Huygens wavelet (top) and a smoothed time integral (bottom). omk-huygens [ER]

would be about 1024 $\times$ 256 or more, but the coarser mesh used here provides a plot of suitable detail). Because of the difficulty in plotting functions that resemble an impulsive doublet, a second plot of the time integral, (with gentle band limiting) is displayed in the lower part of Figure 3.8.

3.3 THE PHASE-SHIFT METHOD

The phase-shift method proceeds straightforwardly by extrapolating downward with $\exp(ik_z z)$ and subsequently evaluating the wavefield at $t = 0$ (the reflectors explode at $t = 0$). Of all the wide-angle methods it most easily incorporates depth variation in velocity. Even the phase angle and obliquity function are correctly included, automatically. Unlike Kirchhoff methods, with this method there is no danger of aliasing the operator.

The phase-shift method begins with a two-dimensional Fourier transform (2D-FT) of the dataset. Then the transformed data values, all in the (ω, k_x)-plane, are